Article

Cell Reports

Phospho-Rasputin Stabilization by Sec16 Is Required for Stress Granule Formation upon Amino Acid Starvation

Graphical Abstract

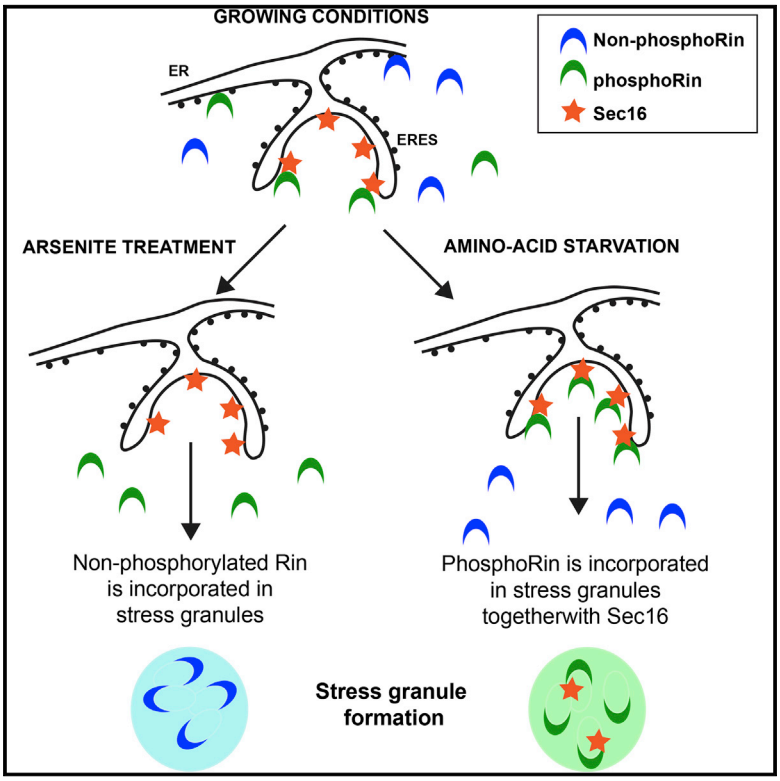

Highlights

- Sec16 is specifically required for stress granule formation upon amino acid starvation
- Sec16 specifically interacts with phosphorylated *Drosophila* G3BP (phosphoRin)
- PhosphoRin is the form required for stress granule formation upon amino acid starvation
- Dephosphorylated Rin is required upon arsenite treatment and does not interact with Sec16

Authors

Angelica Aguilera-Gomez, Margarita Zacharogianni, Marinke M. van Oorschot, ..., Elizabeth R. Gavis, Christian Behrends, Catherine Rabouille

Correspondence

c.rabouille@hubrecht.eu

In Brief

Aguilera-Gomez et al. show that, although stress granules appear similar, the mode of their formation depends on the cellular stress. Contrary to arsenite treatment, the RNA-binding protein Rasputin needs to be phosphorylated and bound to the ERES scaffold Sec16 to lead to the formation of stress granules upon amino acid starvation.

Aguilera-Gomez et al., 2017, Cell Reports *20*, 935–948
July 25, 2017
http://dx.doi.org/10.1016/j.celrep.2017.06.042

Cell Reports
Article

Phospho-Rasputin Stabilization by Sec16 Is Required for Stress Granule Formation upon Amino Acid Starvation

Angelica Aguilera-Gomez,[1] Margarita Zacharogianni,[1,6] Marinke M. van Oorschot,[1] Heide Genau,[2] Rianne Grond,[1] Tineke Veenendaal,[3] Kristina S. Sinsimer,[4,7] Elizabeth R. Gavis,[4] Christian Behrends,[2,8] and Catherine Rabouille[1,3,5,9,*]
[1]Hubrecht Institute-KNAW & University Medical Center (UMC) Utrecht, Uppsalalaan 8, 3584 CT Utrecht, the Netherlands
[2]Institute of Biochemistry II, Medical School Goethe University, 60323 Frankfurt am Main, Germany
[3]Department of Cell Biology, UMC Utrecht, 3584 CT Utrecht, the Netherlands
[4]Department of Molecular Biology, Princeton University, Washington Road, Princeton, NJ 08544, USA
[5]Department of Cell Biology, UMC Groningen, 9713 GZ Groningen, the Netherlands
[6]Present address: Division of Basic Sciences II, Biomedical Research Foundation, Academy of Athens, 115 27 Athens, Greece
[7]Present address: Ethos Health Communications, Inc., Yardley, PA 19067, USA
[8]Present address: Munich Cluster for Systems Neurology (SyNergy), Ludwig-Maximilians-Universität München, 80539 Munich, Germany
[9]Lead Contact
*Correspondence: c.rabouille@hubrecht.eu
http://dx.doi.org/10.1016/j.celrep.2017.06.042

SUMMARY

Most cellular stresses induce protein translation inhibition and stress granule formation. Here, using *Drosophila* S2 cells, we investigate the role of G3BP/Rasputin in this process. In contrast to arsenite treatment, where dephosphorylated Ser142 Rasputin is recruited to stress granules, we find that, upon amino acid starvation, only the phosphorylated Ser142 form is recruited. Furthermore, we identify Sec16, a component of the endoplasmic reticulum exit site, as a Rasputin interactor and stabilizer. Sec16 depletion results in Rasputin degradation and inhibition of stress granule formation. However, in the absence of Sec16, pharmacological stabilization of Rasputin is not enough to rescue the assembly of stress granules. This is because Sec16 specifically interacts with phosphorylated Ser142 Rasputin, the form required for stress granule formation upon amino acid starvation. Taken together, these results demonstrate that stress granule formation is fine-tuned by specific signaling cues that are unique to each stress. These results also expand the role of Sec16 as a stress response protein.

INTRODUCTION

Stress granules are well-studied, cytoplasmic reversible, pro-survival stress assemblies where untranslated free RNAs (resulting from protein translation inhibition) are stored and protected together with RNA-binding proteins, translation initiation factors, and the 40S ribosomal subunits (Anderson and Kedersha, 2008; Protter and Parker, 2016). Stress granule formation has been best investigated in mammalian cells upon different type of stresses, including heat and oxidative stress (Anderson and Kedersha, 2002). This has led to the identification of a number of factors that are essential for their formation, such as the case for Tia-1 (Gilks et al., 2004; Kedersha et al., 1999) and Ras-GAP SH3 domain-binding protein (G3BP1/2, referred to as G3BP hereafter) (Tourrière et al., 2003).

G3BP was first identified in human cells through co-immunoprecipitation with the SH3 domain of RasGAP. However, it has an RNA recognition motif (RRM) toward the C terminus, suggesting that it binds mRNAs. In growing cells, G3BP is normally cytoplasmic; However, after stress induction (especially stress leading to eIF2α phosphorylation; McEwen et al., 2005), it is not only readily recruited to stress granules but also is necessary for their formation (Kedersha et al., 2016; Tourrière et al., 2003; White et al., 2007). Furthermore, G3BP drives stress granule formation when overexpressed in the absence of stress (Tourrière et al., 2003). Importantly, G3BP is phosphorylated on Ser149 during basal conditions, but it needs to be dephosphorylated to drive stress granule assembly triggered by arsenite treatment (Kedersha et al., 2016; Tourrière et al., 2003). Taken together, G3BP is critical for stress granule formation when its Ser149 is dephosphorylated and through its binding to Caprin and the 40S ribosomal subunit. Conversely, G3BP is inhibited when binding to peptidase USP10 (Kedersha et al., 2016).

G3BP also appears to have an important role in disease. First, viruses can exploit G3BP (reviewed in Tsai and Lloyd, 2014). However, G3BP also appears to slow down HIV replication by leading to the sequestration of viral mRNA (Cobos Jiménez et al., 2015). Second, G3BP is overexpressed in gastric cancer (Min et al., 2015) and bone and lung sarcomas (Somasekharan et al., 2015), where it is considered as a marker for poor survival. Strikingly, downregulation of G3BP in cells and in vivo reduces stress granule formation as expected but also tumor invasion and metastasis, showing a clear role for stress granule formation in cancer. Last, G3BP is a target of TDP-43 that is often mutated, mislocalized, and misaccumulated in amyotrophic lateral sclerosis (ALS) (Aulas et al., 2012).

Stress granules are also formed in *Drosophila*, for instance, upon heat stress, arsenite exposure (Farny et al., 2009), and amino acid starvation of *Drosophila* S2 cells (Zacharogianni

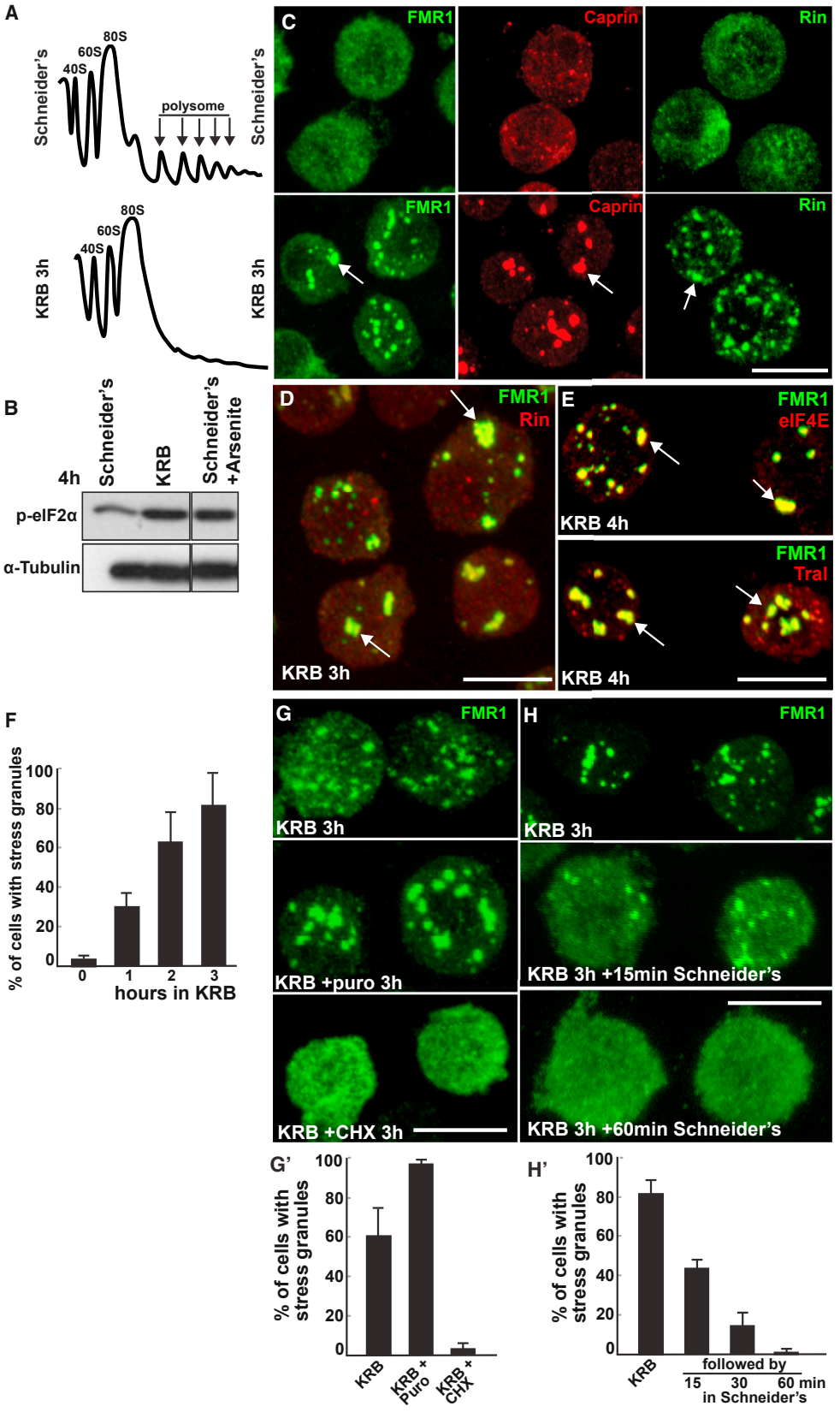

(legend on next page)

et al., 2014). However, the mechanism behind their formation upon this latter stress is not completely understood. Interestingly, amino acid starvation leads to the formation of another recently described stress assembly, the Sec bodies that store and protect most of the COPII subunits and the endoplasmic reticulum exit site (ERES) component Sec16 (Zacharogianni et al., 2014). Importantly, Sec bodies and stress granules are independent structures that are formed at the same time frame of amino acid starvation.

Sec16 is a conserved peripheral membrane protein that tightly localizes and concentrates to the ERES (Connerly et al., 2005; Watson et al., 2006) via a domain that has been mapped to a small arginine-rich region upstream of the conserved central domain (Hughes et al., 2009; Ivan et al., 2008). It binds nearly all COPII subunits and controls at least two aspects of COPII-coated vesicle dynamics (Sprangers and Rabouille, 2015). Sec16 is essential for endoplasmic reticulum (ER) to Golgi transport, especially in *Drosophila* where the absence of Sec16 results in a severe inhibition of protein exit from the ER (Ivan et al., 2008).

Interestingly, Sec16 responds to nutrient stress (Zacharogianni et al., 2011, 2014). In this regard, we have recently shown that Sec16 is a key factor driving Sec body formation upon amino acid starvation that activates the ER-localized dPARP16. In turn, dPARP16 mono-ADP-ribosylates Sec16 on a conserved sequence close to its C terminus (Aguilera-Gomez et al., 2016), and Sec16 modification by dPARP16 is enough to elicit Sec body formation. This demonstrates that Sec16 is a stress response protein that plays an important role in the response to amino acid starvation.

Here we show that the phosphorylation state of the G3BP *Drosophila* ortholog Rasputin (Rin) is differentially required for the formation of stress granules that are formed upon arsenite treatment and amino acid starvation. Whereas stress granule formation upon arsenite treatment requires the non-phosphorylated form of Rin (as is the case for G3BP in mammalian cells), amino acid starvation requires the phosphorylated form. Furthermore, we show that Sec16 specifically interacts with phosphorylated Rin and mediates this differential requirement.

All together, these results provide a link, which to our knowledge has not been reported, between the protein transport from the ER and protein translation. It also explains the specific requirement of Sec16 for stress granule formation upon amino acid starvation, but not other stresses. Furthermore, it enlarges the scope of Sec16 function at the ER by identifying yet a new role in the response to amino acid starvation.

RESULTS

Amino Acid Starvation Induces the Formation of Bona Fide Stress Granules

Amino acid starvation (Incubation in KRB, see the Experimental Procedures and Figures S1A and S1B) induced the inhibition of protein translation (Figure 1A), the phosphorylation of eIF2α (Figure 1B) as strongly as sodium arsenite treatment, and the subsequent formation of stress granules. These were marked by three RNA-binding proteins, FMR1, Caprin, and Rin (Figures 1C and 1D) as well as Tral (Yang et al., 2006) and the initiation factor eIF4E (Figure 1E). Stress granules began to form after 1 hr of starvation, with their number reaching a maximum after 3–4 hr (Figure 1F). They were clearly different from autophagosomes that also formed upon starvation (Figure S1C). Importantly, stress granule formation depended on the presence of ribosome-free mRNAs, as cycloheximide treatment completely blocked their formation in starved cells (Figures 1F and 1F') and cycloheximide washout allowed their formation (data not shown). Conversely, puromycin led to the robust formation of stress granules (Figures 1G and 1G'). Last, they were completely reversible upon 60 min of stress relief (addition of full medium) (Figures 1H and 1H'). This suggests that the stress granules that were formed by amino acid starvation were canonical, as they had the same properties as those formed upon other stresses (Aulas et al., 2017; Farny et al., 2009).

PhosphoRin Is Required for Stress Granule Formation upon Amino Acid Starvation

As mentioned in the Introduction, Rasputin (Rin) is the *Drosophila* ortholog of G3BP and the molecular organization is largely conserved (Figure S2A). So are the amino acid sequences of the NFT2 and RRM domains (Figure S2C). Importantly, Ser149 of G3BP is conserved in Rin (Ser142) (Figure S2B). Furthermore, both proteins harbor a proline-rich intrinsically disordered domain and a glycine rich-domain at the C terminus (Kedersha et al., 2016). Interestingly, as G3BP, Rin overexpression in mammalian cells leads to the formation of stress granules in the absence of stress (Tourrière et al., 2003).

To test the role of Rin in stress granule formation in amino acid-starved *Drosophila* S2 cells, we first depleted it. In the absence of Rin (Figure 2A"), stress granules (marked by FMR1) did not form (Figures 2A and 2A'). We then investigated whether Rin overexpression drives stress granule formation in *Drosophila* S2 cells in the absence of stress. However, this was not the

Figure 1. Amino Acid Starvation Leads to the Formation of Canonical Stress Granules

(A) Polysome profiles of *Drosophila* S2 cells grown in Schneider's and incubated 4 hr in KRB.

(B) Western blot visualization of eIF2α phosphorylation in growing, KRB- and arsenite-treated cells.

(C) Immunofluorescence (IF) visualization of endogenous FMR1, Caprin, and Rin in cells incubated in Schneider's and KRB for 3 hr. Note that stress granules form (arrows).

(D) IF co-localization of FMR1 and Rin. Note that they perfectly co-localize in stress granules (arrows).

(E) IF co-localization of FMR1 and eIF4E and FMR1 and Tral in stress granules (arrows).

(F) Kinetics of stress granule formation (marked by FMR1) in S2 cells incubated in KRB over the indicated time.

(G) IF visualization of FMR1 upon KRB incubation, KRB supplemented with puromycin (puro) and cycloheximide (CHX), quantified in (G'). Note that stress granules do not form upon CHX incubation.

(H) IF visualization of FMR1 upon KRB incubation followed by 15 and 60 min reversion in Schneider's, quantified in (H'). Note that stress granules dissolve rapidly upon stress relief.

Scale bars, 10 μm. Error bar, SEM.

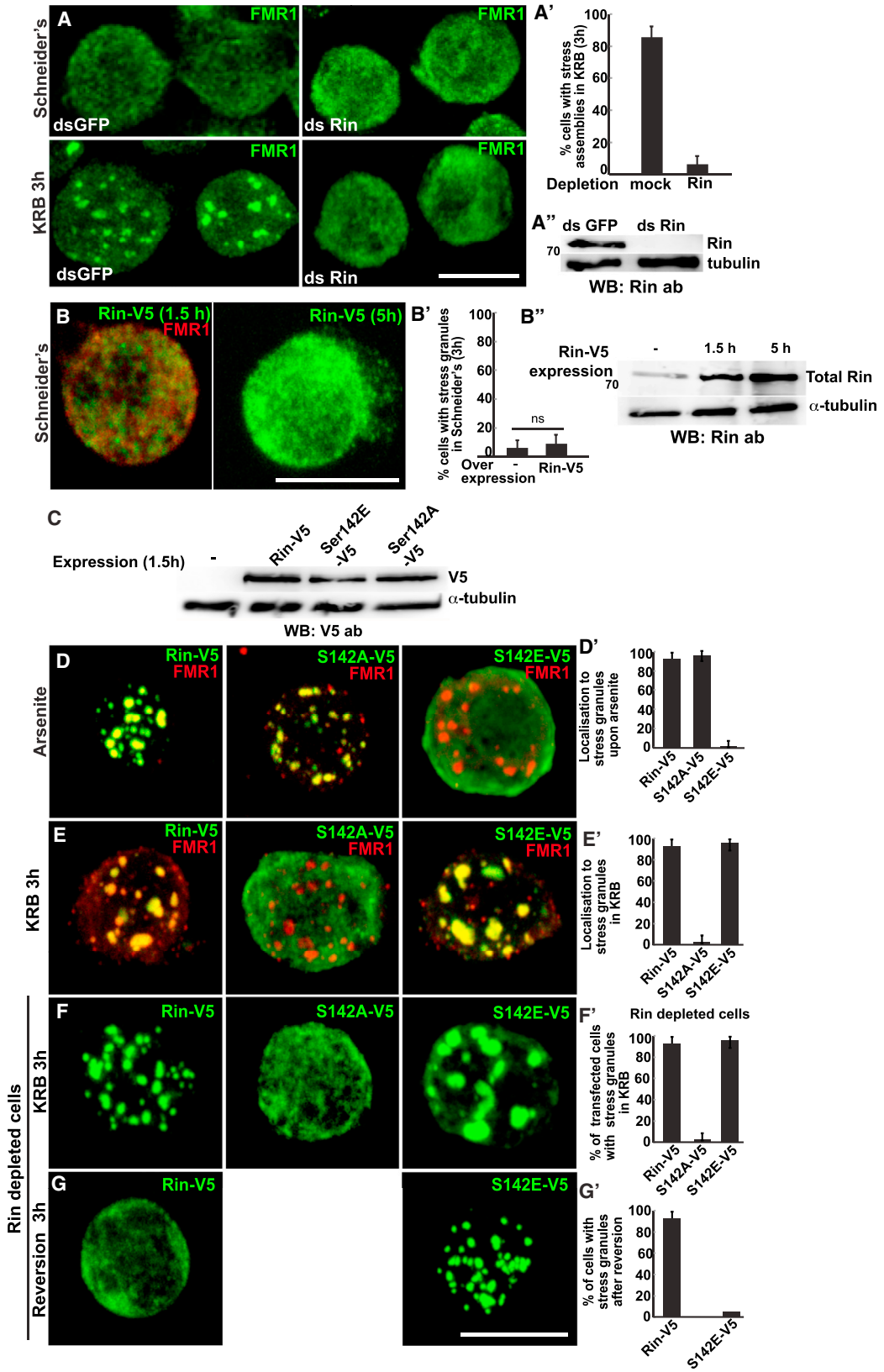

(legend on next page)

case (Figures 2B and 2B'), even after prolonged expression when the total level of Rin clearly increased (Figure 2B''). Taken together, this suggests that Rin is necessary, but not sufficient, to drive the assembly of *Drosophila* stress granules.

As hinted at in the Introduction, S149A, but not S149E, G3BP rescues arsenite-triggered stress granule formation in G3BP-depleted mammalian cells (Tourrière et al., 2003; Kedersha et al., 2016). This shows that, upon arsenite treatment, the stress granule formation-competent form of G3BP is the dephosphorylated form. To test how Rin behaves in S2 cells, we generated phospho-mimetic S142E-V5 and non-phosphorylatable S142A-V5 Rin mutants, overexpressed them in wild-type S2 cells (Figure 2C), and tested their incorporation into stress granules upon arsenite treatment. Only S142A-V5 Rin was incorporated into stress granules, whereas S142E-V5 was completed excluded and remained cytoplasmic (Figures 2D and 2D'). In striking contrast, upon amino acid starvation, S142A-V5 remained cytosolic, whereas S142E-V5 Rin was readily incorporated into stress granules as efficiently as the wild-type Rin (Figures 2E and 2E'). We confirmed this result by expressing the Rin mutants in Rin-depleted cells. Both Rin-V5 and S142E-V5 expression rescued the formation of stress granules in amino acid-starved cells, whereas S142A did not (Figures 2F and 2F'). This shows that, contrary to arsenite treatment, phosphorylated Rin is the competent form for stress granule formation upon amino acid starvation.

Interestingly, S142E-V5 overexpression (Table S1, line 7) led to a 1.7-fold increase in the size of stress granules when compared to Rin-V5 overexpression that resulted in the formation of smaller but more numerous stress granules (Table S1, line 5). This suggests that the dynamics of stress granules might be affected by the inability of Rin to be dephosphorylated. To test this, we assessed the reversibility of the Rin-V5- and S142E-V5-positive stress granules. We found that Rin-V5-positive stress granules are fully reversible, whereas the ones formed by S142E-V5 are not, even after 3 hr of full medium incubation (Figures 2G and 2G'; Table S1, lines 6 and 8). This shows that, upon amino acid starvation, stress granule formation requires the phosphorylated form of Rin, whereas stress granule reversion requires its dephosphorylation.

Taken together, these results show that the formation of stress granules upon both arsenite and amino acid starvation is modulated by different but specific signaling cues. This prompted us to look for factors that are required for stress granule formation specifically upon amino acid starvation, but not upon other stresses.

Sec16 Interacts with Rin

In addition to stress granule formation, amino acid starvation also triggers Sec body formation (Zacharogianni et al., 2014). Importantly, Sec bodies are exclusively formed upon amino acid starvation, not arsenite treatment. Furthermore, although stress granules and Sec bodies are distinct structures, they tend to form in close proximity to each other (Figures 3A–3A''). In this respect, using immunoelectron microscopy, we found a small pool of Sec16 localized inside stress granules (asterisk in Figures 3B and 3B', red circles), although, as reported before, Sec16 bulk is found in Sec bodies (Figure 3B, arrow) (Zacharogianni et al., 2014). This led us to investigate whether Sec16 plays a role in stress granule formation upon amino acid starvation.

To begin to investigate this, we performed a mass spectrometry analysis of proteins co-immunoprecipitated with endogenous Sec16 from cells in growing conditions and upon amino acid starvation. 149 candidate interactors passing the selection criteria (see the Experimental Procedures; Table S2) were pulled down, 62% specifically from starved cells, 17% only from cells in growing conditions, and 21% from both conditions, such as Sec13 (Table S2). All candidates were grouped by 12 gene ontology (GO) terms, including one (RNA-binding proteins) that is functional for stress granule formation to which Rin belongs (Table S2; Figure 3C).

We confirmed that Sec16 binds to Rin using several approaches. First, Sec16 immunoprecipitation followed by western blot clearly showed that Sec16 bound Rin (Figure 3D) in a specific manner, as Caprin and FMR1 were not co-immunoprecipitated (Figure S3A). Second, their interaction was also suggested in physiological conditions where Rin was observed in very close proximity to Sec16, especially at the earlier time point of amino acid starvation (Figure S3B, S3B'). Third, we used an anchor-away strategy, whereby Sec16 tagged with the Ras CAAX motif resulted in its anchoring to the plasma membrane (Aguilera-Gomez et al., 2016). Using full-length Sec16-CAAX, we demonstrated that endogenous Rin is very efficiently recruited to the plasma membrane (Figures 3E and 3J), confirming their interaction.

The C terminus part of Sec16 has been implicated in the stress response (Zacharogianni et al., 2011, 2014), and we tested whether it is also involved in Sec16/Rin interaction. To do this,

Figure 2. Rin S142E, not S142A, Is Incorporated in Stress Granules upon Amino Acid Starvation

(A–A'') IF visualization of FMR1 in mock- (dsGFP) and Rin- (dsRin) depleted S2 cells (A and A'') in growing conditions (Schneider's) and upon amino acid starvation (KRB), quantified in (A').

(B) Note that Rin-V5 overexpression (1.5 and 5 hr) does not induce stress granule formation even though the level of total Rin measured by western blot (using the anti-Rin antibody) increases (B''), quantified in (B').

(C) Western blot (using anti-V5 antibody) assessing the expression level of the V5-tagged Rin constructs used in (D)–(G).

(D, D') IF visualization of FRM1 (red) and overexpressed Rin-V5, S142A-V5, and S142E-V5 upon arsenite treatment for 3 hr (D). Note that S142A-V5 is steadily recruited into stress granule, while S142E is not. Quantified in D'.

(E, E') IF visualization of FRM1 (red) and overexpressed Rin-V5, S142A-V5, and S142E-V5 upon incubation in KRB for 3 hr (E). Note that S142E-V5 is steadily recruited into stress granule, while S142A is not. Quantified in E'.

(F–F') IF visualization of Rin-V5, S142A-V5, and S142E-V5 in cells depleted of endogenous Rin incubated in KRB for 3 hr (F). Note that Rin-V5 and S142E-V5 expression rescues stress granule formation, whereas S142A expression does not. Quantified in F'.

(G–G') IF visualization of Rin-V5 and S142E-V5 in Rin depleted cells after incubation in KRB for 3 hr followed by 3 hr incubation in Schneider's (reversion) (G and quantified in G'). Note that Rin-V5 positive stress granules are completely reverted, whereas S142E positive stress granules are not.

Scale bars, 10 μm. Error bar, SEM.

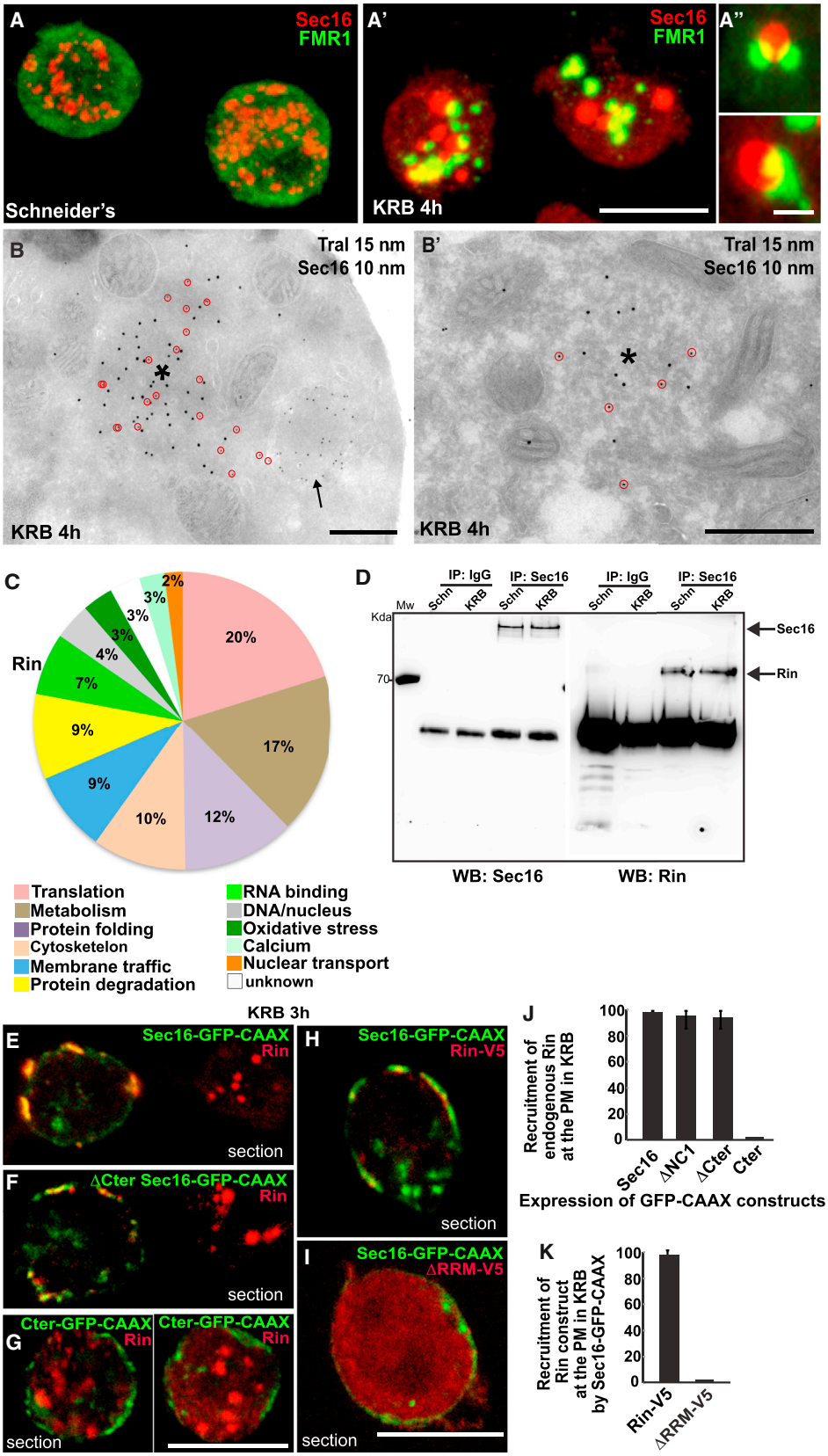

(legend on next page)

we expressed Sec16-GFP-CAAX lacking its C terminus, but Rin was still recruited to the plasma membrane (Figures 3F and 3J). Accordingly, expression of the Sec16 Cter-CAAX did not recruit Rin (Figures 3G and 3J), and Rin was able to form stress granules in the cytoplasm. The N terminus of Sec16 was also not required for Rin binding (Figure S3C; Figure 3J).

We then examined whether the RNA-binding domain (RRM) of Rin is required for Sec16 interaction, by generating a ΔRRM Rin mutant (Figure S2C) and expressing it together with Sec16-GFP-CAAX. This mutant was not recruited to the plasma membrane, suggesting that this domain is important for Sec16/Rin interaction (Figures 3H, 3I, and 3K). Importantly; ΔRRM Rin did not form stress granules. Furthermore, it had a dominant-negative effect as when expressed in wild-type cells; it prevented the formation of stress granules (Figure S3D). Taken together, these results show that Sec16 is a new Rin interactor.

Sec16, but Not Active Secretion, Is Specifically Required for Stress Granule Formation upon Amino Acid Starvation

We then examined whether Sec16 plays a role in stress granule formation specifically induced by amino acid starvation. We starved Sec16-depleted cells, and we found that stress granules are formed 75% less than in mock-depleted cells (Figure 4E), as monitored using Rin (Figure 4A), eIF4E and Tral (Figure 4B), FMR1 (Figure 4C), and Caprin (data not shown). This indicates that Sec16 is a factor required in stress granule formation.

To investigate whether the Sec16 requirement is specific for stress granule formation upon amino acid starvation, we treated Sec16-depleted cells with arsenite (Figures 4D and 4E), heat stress, and ER stress (DTT) (Figure S4A; Figure 4E), and we monitored stress granule formation that was found to be as efficient as in mock-depleted cells. This shows that Sec16 is required for stress granule formation specifically upon amino acid starvation.

Last, we addressed whether the role of Sec16 in stress granule formation is linked to its role in protein exit from the ER by COPII-coated vesicles. To test this, we inhibited COPII vesicle formation by depleting Sar1, but this did not prevent stress granule formation upon amino acid starvation (Figure S4B; Figure 4E). Similarly, COPI-coated vesicle formation and retrograde transport from the Golgi to the ER were also not required, as stress granule formation was insensitive to incubation with brefeldin A (Figure S4C; Figure 4E). Taken together, transport through the early secretory pathway is not required for stress granule formation upon amino acid starvation, and the role for Sec16 in their formation lies somewhere else.

Sec16 Is Required for Rin Stability

We noticed that in Sec16-depleted cells the fluorescence level of Rin was low (Figure 4A). This was confirmed by western blot (Figure 4F), where, in the absence of Sec16, Rin level in amino acid-starved cells was reduced compared to control cells. This appears to be specific because, although FMR1 was partly affected, Caprin and CF68 (CG7185) were not. This result suggests that Sec16 depletion mimics Rin depletion, which, as we have shown above, results in a strong inhibition of stress granule formation (Figures 2A–2A").

There are at least three ways by which Sec16 can contribute to the maintenance of Rin protein level. It could stabilize its mRNA, it could promote its translation, and it could stabilize the Rin protein. To test the first hypothesis, we monitored Rin mRNA upon Sec16 depletion and found that it was not affected (Figure S5A). To test the latter hypothesis (whether Sec16 stabilizes Rin protein), we transfected mock- or Sec16-depleted cells with Rin-V5, and we treated them with or without the proteasome inhibitor MG132. This allowed us to trigger Rin expression acutely for a short period of time and monitor its level. If the reduced level of Rin observed upon Sec16 depletion was due to protein degradation, the addition of MG132 should rescue it.

We first confirmed that Rin-V5 level was also very low in Sec16-depleted cells (Figures 5A and 5B, compare lanes 1 and 2). In the presence of MG132, however, Rin-V5 level was partially restored (Figures 5A and 5B, compare lanes 3 and 4), showing that Sec16 stabilizes Rin at the protein level and protects it against degradation through the proteasome. Furthermore, whereas stress granule formation was inhibited in Sec16-depleted starved cells as reported above, MG132 treatment significantly rescued the formation of stress granules (also positive for FMR1; Figure S5B) in cells expressing Rin-V5 (Figure 5B, arrow; Figure 5E). This demonstrates that Sec16 stabilizes Rin

Figure 3. Sec16 Interacts with Rin

(A) IF visualization of FMR1 (green) and Sec16 (red) in cells in Schneider's (A) and in KRB (A'). Note that Sec bodies (marked by Sec16) and stress granules form in close proximity to each other (A").

(B) Immuno-EM localization of Sec16 (10 nm gold) and Tral (15 nm gold) in ultrathin sections of S2 cells incubated in KRB for 4 hr (B and B'). Note that Sec16 is mostly localized to Sec bodies (arrow) but also populates (red circles) stress granules (asterisks, marked by Tral). Note the mitochondria surrounding stress granules.

(C) Pie chart representation of the 12 gene ontology groups representing the 149 interactors of endogenous Sec16 (see the Experimental Procedures and Table S2).

(D) Western blot visualization of Rin following immunoprecipitation of endogenous Sec16 from growing (Schneider's) and amino acid-starved (KRB 3 hr) S2 cells.

(E–G and J) Confocal sections co-visualizing full-length Sec16-GFP-CAAX (E), ΔCter Sec16-GFP-CAAX (F), and Cter-GFP-CAAX (G) and endogenous Rin (red) upon amino acid starvation (KRB), quantified in (J).

(H, I, and K) Confocal sections co-visualizing Sec16-GFP-CAAX with Rin-V5 (red, H) and with ΔRRM Rin-V5 (red, I) upon amino acid starvation (KRB), quantified in (K). Note that Rin-V5 is efficiently recruited to the plasma membrane by Sec16-CAAX, whereas ΔRRM-V5 is not and also does not form stress granules.

Scale bars, 10 μm. Error bar, SD.

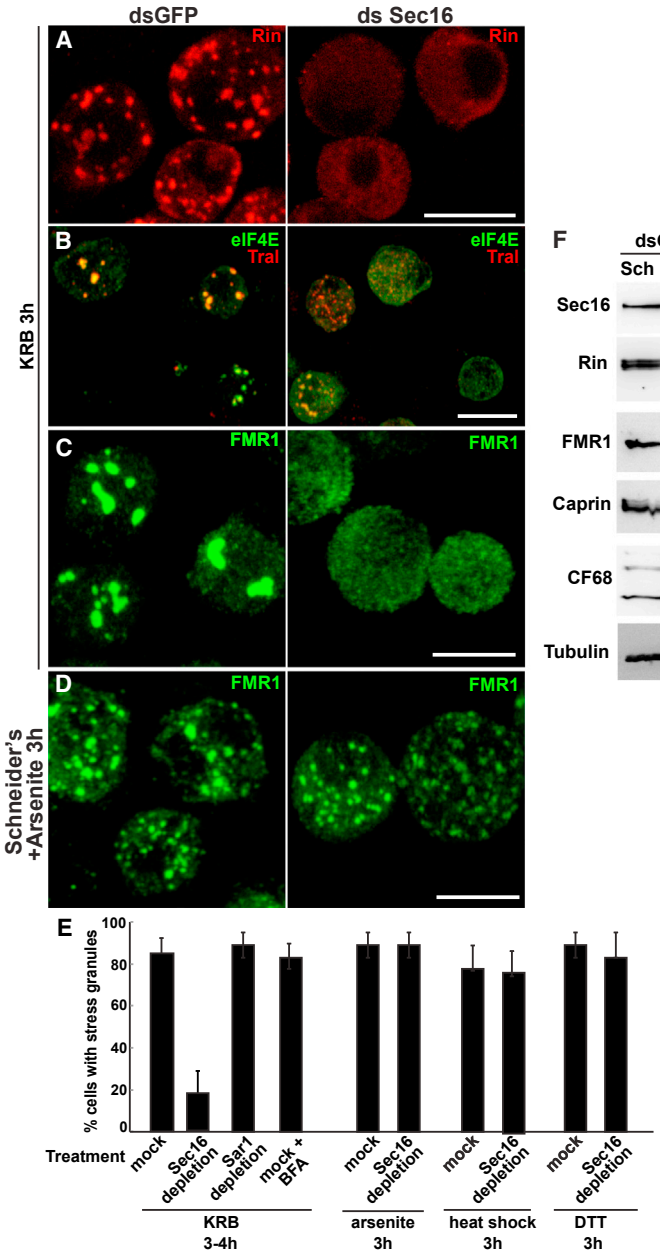

Figure 4. Sec16 Is Required for Stress Granule Formation Specifically upon Amino Acid Starvation

(A–C) IF visualization of endogenous Rin (A), Tral and eIF4E (B), and FMR1 (C) in mock- (dsGFP) and Sec16- (dsSec16) depleted cells upon 3 hr of incubation in KRB. Note that, in the absence of Sec16, stress granules do not form and Rin fluorescence is weak when compared to mock depleted cells.

(D) IF visualization of endogenous FMR1 in mock- and Sec16-depleted cells upon arsenite treatment (3 hr). Note that stress granules form as efficiently in mock- and Sec16-depleted cells.

(E) Quantification of Sec16-depleted cells treated with KRB, arsenite, heat shock, and DTT, expressed in percentage of cell with stress granules.

(F) Western blot of Sec16, Rin, FMR1, Caprin, CF68, and tubulin in mock- and Sec16-depleted cells.

Scale bars, 10 μm. Error bars, SEM.

protein that can then act as a driver for stress granule formation in amino acid-starved cells.

Sec16 Interacts Specifically with PhosphoRin

However, although the level of endogenous Rin was completely recovered upon MG132 incubation of Sec16-depleted cells (Figure 5C), neither Rin (Figure 5D, arrowhead) nor FMR1 (Figure S5B, arrowhead) was recruited to stress granules, whose formation was not rescued (Figure 5E). This suggests that maintaining the level of endogenous Rin is not enough to form stress granules when Sec16 is absent.

Given that Sec16 is specifically required for stress granule formation upon amino acid starvation, but not upon arsenite treatment (Figures 4C and 4D), and that the phosphorylated form of Rin is specifically recruited to stress granules upon amino acid starvation, we reasoned that Sec16 may specifically interact with Rin phosphorylated on Ser142. To test this, we anchored-away Sec16 to the plasma membrane using CAAX (as described in Figure 2), and we expressed the wild-type Rin-V5 and two Rin mutants S142A and S142E upon amino acid starvation. In agreement with our hypothesis, both Rin-V5 and S142E strongly interacted with Sec16, whereas S142A did not (Figures 5F and 5F') and also did not form stress granules (as shown in Figures 2E and 2E').

In striking contrast, none of the Rin forms were recruited to the plasma membrane by Sec16-GFP-CAAX upon arsenite stress (Figures 5G and 5G'). Instead, Rin-V5 and S142A-V5 formed stress granules (red arrows), whereas S142E remained diffuse in the cytoplasm (as shown in Figures 2D and 2D').

Taken together, we show that the Sec16 requirement for stress granule formation upon amino acid starvation is mediated by its specific interaction with phosphoRin, the form that is incorporated into stress granules upon this type of stress.

DISCUSSION

A Specific Role for PhosphoRin in Stress Granule Formation upon Amino Acid Starvation

Stress granules are formed when protein translation initiation is inhibited by cellular stress that leads to eIF2α phosphorylation and the accumulation of untranslated mRNAs (Anderson and Kedersha, 2006; Aulas et al., 2017; Kedersha et al., 2016). Stress

granule components start to coalesce through protein-protein interactions mediated by proteins containing regions of low-complexity sequences and displaying multivalence interactions. This process is facilitated by the presence of accumulating free mRNAs (Molliex et al., 2015; Patel et al., 2015). Accordingly, incubation of stressed cells with cycloheximide, which locks ribosomes to the mRNA, blocks stress granule formation, whereas puromycin stimulates their formation. Stress granule formation is also driven by a number of critical factors, including G3BP. In all these respects, the cytoplasmic foci that are formed in *Drosophila* cells upon amino acid starvation and that are positive for RNA-binding proteins are bona fide stress granules, as they share many features of those found in mammalian cells after arsenite treatment, heat stress, and ER stress (Aulas et al., 2017). Furthermore, we show that Rin, the G3BP *Drosophila* ortholog, is an essential factor for amino acid starvation-driven stress granules.

However, stress granule formation displays a certain level of heterogeneity. First, some of the signaling cues inducing their formation appear to be different. For instance, although eIF2α phosphorylation is required for arsenite-triggered stress granule formation in *Drosophila* cells, this phosphorylation is not necessary for their formation upon heat stress (Farny et al., 2009). Second, mammalian stress granules that are formed upon different stresses appear to have slightly different content, at least in HAP1 cells (Aulas et al., 2017). Third, stress granules display different material properties. Yeast stress granules possess a solid core made of components that exchange slowly and less dynamically (Buchan and Parker, 2009; Jain et al., 2016), whereas mammalian stress granules have liquid droplet properties (Molliex et al., 2015; Nott et al., 2015; Patel et al., 2015). This is also reflected by the fact that stress granules contain diverse proteomes (Jain et al., 2016).

Remarkably, here we show the phosphorylation status of Rin dictates its differential recruitment to stress granules formed upon arsenite treatment and amino acid starvation. Phosphorylated Rin (on Ser142) is instrumental for stress granule formation upon amino acid starvation, whereas arsenite-driven stress granules require dephosphorylated Rin (as for G3BP in mammalian cells). To the best of our knowledge, this is the first example that clearly demonstrates this differential usage. This further documents that stress granules are more complex and variable than previously anticipated and not just a temporal storage of stalled ribonucleoprotein particles (RNPs).

PhosphoRin Specifically Interacts with Sec16, a Key ERES Component

What determines the use for phosphoRin versus non-phosphoRin in stress granule formation upon different stresses is not fully understood, but the first clue is the discovery that the large hydrophilic ERES protein Sec16 specifically interacts with phosphoRin.

Sec16 adds to the lengthening list of factors modulating stress granule formation via their interaction with G3BP, such as Caprin (Kedersha et al., 2016; Solomon et al., 2007), TDP43 (Aulas et al., 2012), and Usp10 (Panas et al., 2015; Soncini et al., 2001; Kedersha et al., 2016). In addition, YB-1 promotes the translation of G3BP1 mRNA (Somasekharan et al., 2015). Sec16 depletion leads to a reduced level of total Rin, but the remaining Rin pool is enough to lead to stress granule formation upon arsenite treatment, heat stress, and ER stress.

Interestingly, Rin level is further reduced when Sec16-depleted cells are amino acid starved. Thus, Sec16 depletion upon amino acid starvation mimics Rin depletion, explaining the inhibition of stress granule formation upon this stress. This suggests that Sec16 protects Rin against proteasome degradation. It is very often the case that proteins in a complex stabilize each other and that when one partner is absent the other is degraded. However, Rin depletion does not affect Sec16 stability. Sec16 has, therefore, an active role in protecting Rin, perhaps by preventing Rin ubiquitination, a signal for degradation through the proteasome.

However, although proteasome inhibition restores Rin level in starved Sec16-depleted cells, this is not enough to recover stress granule formation. This suggests that Sec16 has an additional role. Given that Sec16 specifically interacts with phosphoRin, this interaction appears necessary not only to protect and stabilize phosphoRin but also to facilitate the role of phosphoRin in stress granule formation upon amino acid starvation. It is possible that the Sec16/phosphoRin complex is recruited to stress granules and/or that Sec16 allows Rin to bind another stress granule partner. In any case, this is strictly specific for amino acid starvation.

Indeed, phosphoRin is the form that is specifically required for stress granule formation upon amino acid starvation. Upon arsenite treatment, the dephosphorylated form of Rin is the form required for stress granule formation both in *Drosophila* (our results and in mammalian cells; Kedersha et al., 2016; Tourrière et al., 2003). This is mirrored by the role of Sec16 that is specifically required for stress granule formation upon amino acid starvation, but not upon heat stress, ER stress, and arsenite treatment. Accordingly, Sec16 does not interact with dephosphorylated Rin.

Does Sec16 have a role in Rin phosphorylation? Rin phosphorylation could take place in the cytoplasm independently of Sec16 that would then recognize phosphoRin and stabilize it. Alternatively, Sec16 could contribute to Rin phosphorylation by acting as a scaffold for the kinase required for Rin phosphorylation. This kinase, which we propose is likely to be (hyper-)activated by amino acid starvation, remains to be identified.

Sec16 Links the Inhibition of Protein Translation and Protein Transport

Why does amino acid starvation require this specific Sec16/phosphoRin interaction? Why is an ERES component functionally linked to stress granule formation specifically upon this stress? It is likely that this specific interaction elicits the formation of unique stress granules, perhaps storing mRNAs encoding proteins key for survival upon starvation and fitness upon stress relief. In this respect, stress granules formed during amino acid starvation contain the P-body component Tral that is not found in those formed upon heat shock (Jevtov et al., 2015). Interestingly, Tral has been shown to bind mRNAs encoding COPII subunits (Wilhelm et al., 2005), and it is possible that other mRNAs encoding or secretory pathway components may be sequestered and protected inside these stress granules. This would reflect a type of multiplexing that has been observed in neurons

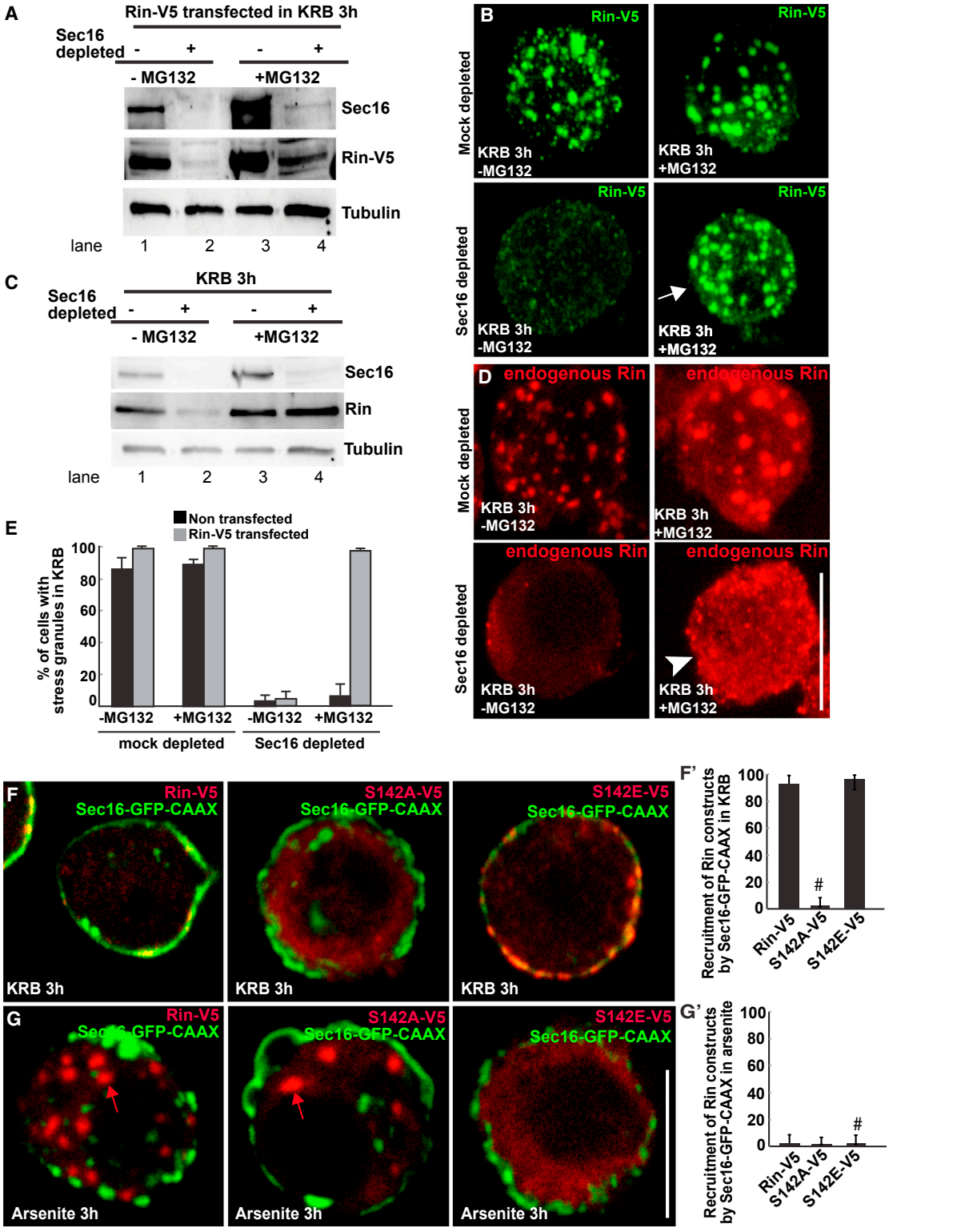

Figure 5. Sec16 Prevents Rin Degradation by the Proteasome

(A) Western blot visualization of Rin-V5 (using an anti-V5 antibody) transfected in mock- and Sec16-depleted cells incubated in Schneider's and KRB (3 hr), supplemented or not by MG132. Note that MG132 incubation partially rescues Rin-V5 protein level.

(B) IF visualization of Rin-V5 transfected in mock- and Sec16-depleted cells in KRB, supplemented or not with MG132. Note that MG132 incubation completely rescues stress granule formation in Sec16-depleted cells.

(legend continued on next page)

(Carson et al., 2008; Smith et al., 2014). Conversely, as ER-translated mRNAs (possibly encoding secretory proteins required in stress recovery) are proposed to escape sequestration to stress granules (Unsworth et al., 2010), Sec16 interaction with stress granule components might restrict stress granule formation to specific sites away from these mRNAs.

Last, the enrichment of phosphoRin (and the presence of Sec16) in amino acid starvation-driven stress granules might change their material properties and, consequently, their dynamics. This is suggested by the large size of the S142E-positive stress granules and by their poor reversibility. Consequently, the exchange of components with the surrounding cytoplasm might be reduced in phosphoRin-based stress granules when compared to stress granules that depend on the dephosphorylated form of Rin (and G3BP). This is supported by fluorescence recovery after photobleaching (FRAP) experiments. G3BP-positive arsenite-driven stress granules show full recovery in less than 1 s (Patel et al., 2015), whereas the recovery of stress granules formed upon amino acid starvation is an order of magnitude slower (Zacharogianni et al., 2014). The biological relevance of this difference is, however, not fully understood.

Overall, the results presented here are in congruence with evidence of the link among protein translation, RNA metabolism, and the secretory pathway. Stress granules are formed in response to ER stress (McEwen et al., 2005; our data). P-bodies also localize in close proximity to the ER and increase in number in response to ER homeostasis perturbations and in Arf1 yeast mutant (Kilchert et al., 2010). Last, ER-resident proteins are shown to regulate P-body formation in yeast (Weidner et al., 2014).

Sec16, a Versatile Scaffold Protein in Basal and Stressed Conditions

Our results provide further evidences of the versatility of Sec16. In growing conditions, mammalian Sec16 exists as two isoforms that are both localized to the ERES (Watson et al., 2006; Bhattacharyya and Glick, 2007) but have non-redundant functions in humans. Whereas Sec16A is classically required for the ER exit of proteins destined to the Golgi and the plasma membrane (Sprangers and Rabouille, 2015), Sec16B specializes in transport to peroxisomes (Budnik et al., 2011; Yonekawa et al., 2011). Furthermore, Sec16 exons have been shown to be alternatively spliced upon T cell activation (Martinez et al., 2012), and increased expression of the Sec16 isoform containing exon 29 leads to an increased number of ERESs and more efficient COPII transport in activated T cells (Wilhelmi et al., 2016). In this regard, Sec16 is also specifically phosphorylated by ERK2 upon serum stimulation in mammalian cells, leading to an increase in the number of ERESs and a larger secretory capacity (Farhan et al., 2010). Sec16 also interacts with LKKR2, albeit in a kinase activity-independent fashion (Cho et al., 2014), and with ULK (Atg1) in non-stressed conditions (Joo et al., 2016).

Sec16 also plays key roles in the response to stress, for instance, to ER stress where it appears to mediate the Golgi bypass of transmembrane proteins (Piao et al., 2017), but also to nutrient stress (Zacharogianni et al., 2011). Amino acid starvation is an interesting stress as it triggers the formation of two stress assemblies in the same time frame, both requiring Sec16 but in two different manners: The first, the MARylation of Sec16 on its C terminus by ER-localized dPARP16, is an event that is enough to trigger the formation of Sec bodies (Aguilera-Gomez et al., 2016). The second is the Sec16 interaction and stabilization of phosphoRin, leading to the formation of stress granules. Interestingly, neither of these is linked to the Sec16 role in protein exit from the ER or COPII-coated vesicle dynamics (Zacharogianni et al., 2014; this work).

Taken together, this demonstrates the versatility and capacity of the large scaffold protein Sec16 to regulate very diverse cellular processes, many of them pro-survival. Therefore, more Sec16 interactors need to be identified and studied.

EXPERIMENTAL PROCEDURES

Cell Culture, Amino Acid Starvation, Depletions, and Transfections

Drosophila S2 cells (mycoplasma free) were cultured in Schneider's medium (Sigma) supplemented with 10% insect-tested fetal bovine serum at 26°C, as described previously (Kondylis and Rabouille, 2003; Kondylis et al., 2007). Amino acid starvation of cells for 3 or 4 hr was performed using Krebs Ringer's Bicarbonate buffer (KRB: 10 mM D(+) Glucose, 0.5 mM MgCl2, 4.5 mM KCl, 121 mM NaCl, 0.7 mM Na2HPO4, 1.5 mM NaH2PO4, and 15 mM sodium bicarbonate) at pH 7.4 (Aguilera-Gomez et al., 2016; Zacharogianni et al., 2014). Note that the starvation buffer did not contain any dialysed fetal bovine serum (FBS), but the addition of this serum did not alter stress granule formation (see Figure S1A).

Wild-type *Drosophila* S2 cells were depleted by double-stranded (ds)RNAi, as previously described (Aguilera-Gomez et al., 2016). Cells were analyzed after incubation with dsRNAs for 5 days, typically leading to depletion in more than 90% of the cells.

Transient transfections of posttranslational modifications (PMT) constructs (see below) were performed using Effectene transfection reagent (301425,

(C) Western blot visualization of endogenous Rin in mock- and Sec16-depleted cells in KRB, supplemented or not with MG132. Note that MG132 incubation completely rescues endogenous Rin protein level.

(D) IF visualization of endogenous Rin in mock- and Sec16-depleted cells in KRB, supplemented or not with MG132. Note that MG132 incubation rescues endogenous Rin protein level (C), but it does not rescue stress granule formation.

(E) Quantification of stress granule formation in Rin-V5 transfected and non-transfected cells in mock- and Sec16-depleted cells incubated in KRB, supplemented or not with MG132, expressed in percentage of cell profiles with stress granules.

(F) Confocal section co-visualizing full-length Sec16-GFP-CAAX in cells expressing Rin-V5, S142A-V5, and S142E-V5 Rin mutants upon amino acid starvation (KRB) (F), quantified in F' (expressed as percentage of Sec16-GFP-CAAX transfected cells). Note that both Rin-V5 and S142E-V5 steadily localize at the plasma membrane in cells expressing Sec16-GFP-CAAX, whereas S142A remains dispersed in the cytoplasm (marked by # in F').

(G) Confocal section co-visualizing full-length Sec16-GFP-CAAX in cells expressing Rin-V5, S142A-V5, and S142E-V5 Rin mutants upon arsenite treatment (G), quantified in G' (expressed as percentage of Sec16-GFP-CAAX transfected cells). Note that none of the Rin variants are recruited by Sec16-GFP-CAAX. Furthermore, in agreement with Figures 2E and 2F, Rin-V5 and S142A form stress granules (red arrows). In contrast, S142E remains diffuse in the cytoplasm (marked by # in G').

Scale bar, 10 μm. Error bar, SD.

QIAGEN) according to the manufacturer's instructions. Expression was induced 48 hr after transfection with 1 mM CuSO4 for 1.5 hr (Zacharogianni and Rabouille, 2013).

Antibodies

The antibodies used were as follows: Rabbit polyclonal anti-Sec16 (Ivan et al., 2008) 1:800 immunofluorescence (IF), 1:2,500 western blot (WB); Mouse monoclonal anti-V5 (Thermo Fisher Scientific 46-0705, 1:500 IF); Mouse monoclonal anti-V5 (Life Technologies R960, 1:500 IF, 1:2,000 WB followed by horseradish peroxidase (HRP)-conjugated sheep-anti-mouse HRP Na931, GE Healthcare, 1:2,000); Mouse monoclonal anti-FMR1 (RRID: AB_528251, DSHB supernatant clone 5A11, 1:800 IF, 1:2,000 WB); Rabbit anti-Caprin (1:500 IF, 1:2,000 WB; Reich and Papoulas, 2012); Rabbit polyclonal anti-phospho-eIF2α (S51) (Cell Signaling Technology 9721s, 1:1,000 WB); anti-Tral (gift from A. Nakamura, 1:200 IF); rat anti-eIF4E (gift from A. Nakamura, 1:200 IF, with methanol fixation); Mouse monoclonal anti-α-tubulin (Sigma T5168, 1:100,000 WB); and Rabbit polyclonal anti-CF68 (CG7185, gift from Z. Dominski).

The Rabbit polyclonal anti-Rin is described in the Supplemental Experimental Procedures and Figure S2D and was used at 1:500.

PMT-DNA Constructs and dsRNAs

All the primers used for generating the DNA constructs and RNAi probes and the procedure are included in the Supplemental Experimental Procedures.

IF and Immunoelectron Microscopy

Drosophila S2 cells were plated on glass coverslips, treated as described, fixed in 4% paraformaldehyde (PFA) in PBS for 20 min, and processed for IF as previously described (Kondylis et al., 2007; Zacharogianni and Rabouille, 2013). Samples were viewed under a Leica SPE confocal microscope using a 63× oil lens and two to four times zoom; 14 to 20 planes were projected to capture the whole cell that is displayed unless indicated otherwise. Unless otherwise mentioned, profiles shown are projections of the whole cell profile.

The immunoelectron microscopy (immuno-EM) of FRM1, TRAL, and Sec16 was performed as described previously (Kondylis et al., 2007; van Donselaar et al., 2007) on ultrathin frozen section (70 nm) of S2 cells that had been amino acid starved for 3 hr.

Immunoprecipitation and Mass Spectrometry

For Sec16 immunoprecipitation, 200–300 million S2 cells were grown and starved in Krebs Ringer's Bicarbonate buffer (KRB) for 4 hr. Cell lysate was prepared by incubating cells for 20 min on ice in lysis buffer (10% glycerol, 1% Triton X-100, 50 mM TrisHCl [pH 7.5], 150 mM NaCl, 50 mM NaF, 25 mM Na_2-glycerophosphate, 1 mM Na_2VO_4, 5 mM EDTA, and tablet protease inhibitors tablet [Roche]). Protein A bead slurry was washed with lysis buffer and incubated for 1 hr at 4°C with 20 μg control IgG and anti Sec16 IgG. Subsequently, the beads where incubated for 2 hr at 4°C with cell lysate. After washing with lysis buffer, beads where boiled for 10 min in sample buffer followed by SDS-PAGE, and western blot was performed.

Mass spectrometry is described in the Supplemental Experimental Procedures. To be scored as Sec16-interacting proteins, candidates were required to (1) be present in at least two experiments (of four biological replicates), with at least two peptides per experiment and experimental conditions (growing and/or starvation); and (2) have an intensity of $\log_2$ (IgG:SEC16) $\geq$1 or, in cases were proteins were not found in IgG control, have an intensity >0. See Table S2 reporting the frequency of identification and the growth conditions. Both categories are color coded and sortable.

Heat Stress, Arsenite, and DTT Treatments

Heat stress was performed on 2 × 10^6 *Drosophila* S2 cells in an oven at 37°C (Thermo Electron) for 3 hr as described in Jevtov et al. (2015). Treatments with cycloheximide (10 μM) and puromycin (10 μg/mL), NaAsO2 (0.5 mM), and DTT (2.0 mM, stock in DMSO) were performed at 26°C for 3 hr.

Polysome Profiles

Polysome profiles were generated as described in Pereboom et al. (2011).

Quantification and Statistics

Two to five biological replicates were performed per experiment. For IF of depleted or treated cells, at least four fields per experiment were analyzed comprising at least 50 cells. For transfected cells, at least 30 cells were analyzed. Results are expressed as SD and SEM.

SUPPLEMENTAL INFORMATION

Supplemental Information includes Supplemental Experimental Procedures, five figures, and two tables and can be found with this article online at http://dx.doi.org/10.1016/j.celrep.2017.06.042.

AUTHOR CONTRIBUTIONS

Conceptualization, A.A.-G., M.Z., and C.R.; Methodology, A.A.-G., M.Z., M.v.O., H.G., R.G., T.V., and C.B.; Formal Analysis, A.A.-G., M.Z., C.R., and C.B.; Resources, K.S.S. and E.A.G.; Writing, Review & Editing, C.R. and A.A.-G.; Supervision, C.R., C.B., and E.A.G.

ACKNOWLEDGMENTS

The polysomes profiles were generated by the group of Alyson McInnes at the Hubrecht Institute. Financial support for this paper was provided by the Hubrecht Institute of the KNAW and a grant from NWO (822-020-016 to C.R.). Work in the Behrends lab is supported by the Deutsche Forschungsgemeinschaft within the framework of EXC 1010 SyNergy and SFB1177. Work in the Gavis lab was supported by grant R01 GM061107 from the NIH.

Received: December 22, 2016
Revised: April 22, 2017
Accepted: June 16, 2017
Published: July 25, 2017; corrected online: August 21, 2017

REFERENCES

Aguilera-Gomez, A., van Oorschot, M.M., Veenendaal, T., and Rabouille, C. (2016). In vivo vizualisation of mono-ADP-ribosylation by dPARP16 upon amino-acid starvation. eLife *5*, e21475.

Anderson, P., and Kedersha, N. (2002). Stressful initiations. J. Cell Sci. *115*, 3227–3234.

Anderson, P., and Kedersha, N. (2006). RNA granules. J. Cell Biol. *172*, 803–808.

Anderson, P., and Kedersha, N. (2008). Stress granules: the Tao of RNA triage. Trends Biochem. Sci. *33*, 141–150.

Aulas, A., Stabile, S., and Vande Velde, C. (2012). Endogenous TDP-43, but not FUS, contributes to stress granule assembly via G3BP. Mol. Neurodegener. *7*, 54.

Aulas, A., Fay, M.M., Lyons, S.M., Achorn, C.A., Kedersha, N., Anderson, P., and Ivanov, P. (2017). Stress-specific differences in assembly and composition of stress granules and related foci. J. Cell Sci. *130*, 927–937.

Bhattacharyya, D., and Glick, B.S. (2007). Two mammalian Sec16 homologues have nonredundant functions in endoplasmic reticulum (ER) export and transitional ER organization. Mol. Biol. Cell *18*, 839–849.

Buchan, J.R., and Parker, R. (2009). Eukaryotic stress granules: the ins and outs of translation. Mol. Cell *36*, 932–941.

Budnik, A., Heesom, K.J., and Stephens, D.J. (2011). Characterization of human Sec16B: indications of specialized, non-redundant functions. Sci. Rep. *1*, 77.

Carson, J.H., Gao, Y., Tatavarty, V., Levin, M.K., Korza, G., Francone, V.P., Kosturko, L.D., Maggipinto, M.J., and Barbarese, E. (2008). Multiplexed RNA trafficking in oligodendrocytes and neurons. Biochim. Biophys. Acta *1779*, 453–458.

Cho, H.J., Yu, J., Xie, C., Rudrabhatla, P., Chen, X., Wu, J., Parisiadou, L., Liu, G., Sun, L., Ma, B., et al. (2014). Leucine-rich repeat kinase 2 regulates Sec16A at ER exit sites to allow ER-Golgi export. EMBO J. *33*, 2314–2331.

Cobos Jiménez, V., Martinez, F.O., Booiman, T., van Dort, K.A., van de Klundert, M.A., Gordon, S., Geijtenbeek, T.B., and Kootstra, N.A. (2015). G3BP1 restricts HIV-1 replication in macrophages and T-cells by sequestering viral RNA. Virology *486*, 94–104.

Connerly, P.L., Esaki, M., Montegna, E.A., Strongin, D.E., Levi, S., Soderholm, J., and Glick, B.S. (2005). Sec16 is a determinant of transitional ER organization. Curr. Biol. *15*, 1439–1447.

Farhan, H., Wendeler, M.W., Mitrovic, S., Fava, E., Silberberg, Y., Sharan, R., Zerial, M., and Hauri, H.P. (2010). MAPK signaling to the early secretory pathway revealed by kinase/phosphatase functional screening. J. Cell Biol. *189*, 997–1011.

Farny, N.G., Kedersha, N.L., and Silver, P.A. (2009). Metazoan stress granule assembly is mediated by P-eIF2alpha-dependent and -independent mechanisms. RNA *15*, 1814–1821.

Gilks, N., Kedersha, N., Ayodele, M., Shen, L., Stoecklin, G., Dember, L.M., and Anderson, P. (2004). Stress granule assembly is mediated by prion-like aggregation of TIA-1. Mol. Biol. Cell *15*, 5383–5398.

Hughes, H., Budnik, A., Schmidt, K., Palmer, K.J., Mantell, J., Noakes, C., Johnson, A., Carter, D.A., Verkade, P., Watson, P., and Stephens, D.J. (2009). Organisation of human ER-exit sites: requirements for the localisation of Sec16 to transitional ER. J. Cell Sci. *122*, 2924–2934.

Ivan, V., de Voer, G., Xanthakis, D., Spoorendonk, K.M., Kondylis, V., and Rabouille, C. (2008). Drosophila Sec16 mediates the biogenesis of tER sites upstream of Sar1 through an arginine-rich motif. Mol. Biol. Cell *19*, 4352–4365.

Jain, S., Wheeler, J.R., Walters, R.W., Agrawal, A., Barsic, A., and Parker, R. (2016). ATPase-Modulated Stress Granules Contain a Diverse Proteome and Substructure. Cell *164*, 487–498.

Jevtov, I., Zacharogianni, M., van Oorschot, M.M., van Zadelhoff, G., Aguilera-Gomez, A., Vuillez, I., Braakman, I., Hafen, E., Stocker, H., and Rabouille, C. (2015). TORC2 mediates the heat stress response in Drosophila by promoting the formation of stress granules. J. Cell Sci. *128*, 2497–2508.

Joo, J.H., Wang, B., Frankel, E., Ge, L., Xu, L., Iyengar, R., Li-Harms, X., Wright, C., Shaw, T.I., Lindsten, T., et al. (2016). The Noncanonical Role of ULK/ATG1 in ER-to-Golgi Trafficking Is Essential for Cellular Homeostasis. Mol. Cell *62*, 982.

Kedersha, N.L., Gupta, M., Li, W., Miller, I., and Anderson, P. (1999). RNA-binding proteins TIA-1 and TIAR link the phosphorylation of eIF-2 alpha to the assembly of mammalian stress granules. J. Cell Biol. *147*, 1431–1442.

Kedersha, N., Panas, M.D., Achorn, C.A., Lyons, S., Tisdale, S., Hickman, T., Thomas, M., Lieberman, J., McInerney, G.M., Ivanov, P., and Anderson, P. (2016). G3BP-Caprin1-USP10 complexes mediate stress granule condensation and associate with 40S subunits. J. Cell Biol. *212*, 845–860.

Kilchert, C., Weidner, J., Prescianotto-Baschong, C., and Spang, A. (2010). Defects in the secretory pathway and high Ca2+ induce multiple P-bodies. Mol. Biol. Cell *21*, 2624–2638.

Kondylis, V., and Rabouille, C. (2003). A novel role for dp115 in the organization of tER sites in Drosophila. J. Cell Biol. *162*, 185–198.

Kondylis, V., van Nispen tot Pannerden, H.E., Herpers, B., Friggi-Grelin, F., and Rabouille, C. (2007). The golgi comprises a paired stack that is separated at G2 by modulation of the actin cytoskeleton through Abi and Scar/WAVE. Dev. Cell *12*, 901–915.

Martinez, N.M., Pan, Q., Cole, B.S., Yarosh, C.A., Babcock, G.A., Heyd, F., Zhu, W., Ajith, S., Blencowe, B.J., and Lynch, K.W. (2012). Alternative splicing networks regulated by signaling in human T cells. RNA *18*, 1029–1040.

McEwen, E., Kedersha, N., Song, B., Scheuner, D., Gilks, N., Han, A., Chen, J.J., Anderson, P., and Kaufman, R.J. (2005). Heme-regulated inhibitor kinase-mediated phosphorylation of eukaryotic translation initiation factor 2 inhibits translation, induces stress granule formation, and mediates survival upon arsenite exposure. J. Biol. Chem. *280*, 16925–16933.

Min, L., Ruan, Y., Shen, Z., Jia, D., Wang, X., Zhao, J., Sun, Y., and Gu, J. (2015). Overexpression of Ras-GTPase-activating protein SH3 domain-binding protein 1 correlates with poor prognosis in gastric cancer patients. Histopathology *67*, 677–688.

Molliex, A., Temirov, J., Lee, J., Coughlin, M., Kanagaraj, A.P., Kim, H.J., Mittag, T., and Taylor, J.P. (2015). Phase separation by low complexity domains promotes stress granule assembly and drives pathological fibrillization. Cell *163*, 123–133.

Nott, T.J., Petsalaki, E., Farber, P., Jervis, D., Fussner, E., Plochowietz, A., Craggs, T.D., Bazett-Jones, D.P., Pawson, T., Forman-Kay, J.D., and Baldwin, A.J. (2015). Phase transition of a disordered nuage protein generates environmentally responsive membraneless organelles. Mol. Cell *57*, 936–947.

Panas, M.D., Schulte, T., Thaa, B., Sandalova, T., Kedersha, N., Achour, A., and McInerney, G.M. (2015). Viral and cellular proteins containing FGDF motifs bind G3BP to block stress granule formation. PLoS Pathog. *11*, e1004659.

Patel, A., Lee, H.O., Jawerth, L., Maharana, S., Jahnel, M., Hein, M.Y., Stoynov, S., Mahamid, J., Saha, S., Franzmann, T.M., et al. (2015). A Liquid-to-Solid Phase Transition of the ALS Protein FUS Accelerated by Disease Mutation. Cell *162*, 1066–1077.

Pereboom, T.C., van Weele, L.J., Bondt, A., and MacInnes, A.W. (2011). A zebrafish model of dyskeratosis congenita reveals hematopoietic stem cell formation failure resulting from ribosomal protein-mediated p53 stabilization. Blood *118*, 5458–5465.

Piao, H., Kim, J., Noh, S.H., Kweon, H.S., Kim, J.Y., and Lee, M.G. (2017). Sec16A is critical for both conventional and unconventional secretion of CFTR. Sci. Rep. *7*, 39887.

Protter, D.S., and Parker, R. (2016). Principles and Properties of Stress Granules. Trends Cell Biol. *26*, 668–679.

Reich, J., and Papoulas, O. (2012). Caprin controls follicle stem cell fate in the Drosophila ovary. PLoS ONE *7*, e35365.

Smith, R., Rathod, R.J., Rajkumar, S., and Kennedy, D. (2014). Nervous translation, do you get the message? A review of mRNPs, mRNA-protein interactions and translational control within cells of the nervous system. Cell. Mol. Life Sci. *71*, 3917–3937.

Solomon, S., Xu, Y., Wang, B., David, M.D., Schubert, P., Kennedy, D., and Schrader, J.W. (2007). Distinct structural features of caprin-1 mediate its interaction with G3BP-1 and its induction of phosphorylation of eukaryotic translation initiation factor 2alpha, entry to cytoplasmic stress granules, and selective interaction with a subset of mRNAs. Mol. Cell. Biol. *27*, 2324–2342.

Somasekharan, S.P., El-Naggar, A., Leprivier, G., Cheng, H., Hajee, S., Grunewald, T.G., Zhang, F., Ng, T., Delattre, O., Evdokimova, V., et al. (2015). YB-1 regulates stress granule formation and tumor progression by translationally activating G3BP1. J. Cell Biol. *208*, 913–929.

Soncini, C., Berdo, I., and Draetta, G. (2001). Ras-GAP SH3 domain binding protein (G3BP) is a modulator of USP10, a novel human ubiquitin specific protease. Oncogene *20*, 3869–3879.

Sprangers, J., and Rabouille, C. (2015). SEC16 in COPII coat dynamics at ER exit sites. Biochem. Soc. Trans. *43*, 97–103.

Tourrière, H., Chebli, K., Zekri, L., Courselaud, B., Blanchard, J.M., Bertrand, E., and Tazi, J. (2003). The RasGAP-associated endoribonuclease G3BP assembles stress granules. J. Cell Biol. *160*, 823–831.

Tsai, W.C., and Lloyd, R.E. (2014). Cytoplasmic RNA Granules and Viral Infection. Annu. Rev. Virol. *1*, 147–170.

Unsworth, H., Raguz, S., Edwards, H.J., Higgins, C.F., and Yagüe, E. (2010). mRNA escape from stress granule sequestration is dictated by localization to the endoplasmic reticulum. FASEB J. *24*, 3370–3380.

van Donselaar, E., Posthuma, G., Zeuschner, D., Humbel, B.M., and Slot, J.W. (2007). Immunogold labeling of cryosections from high-pressure frozen cells. Traffic *8*, 471–485.

Watson, P., Townley, A.K., Koka, P., Palmer, K.J., and Stephens, D.J. (2006). Sec16 defines endoplasmic reticulum exit sites and is required for secretory cargo export in mammalian cells. Traffic *7*, 1678–1687.

Weidner, J., Wang, C., Prescianotto-Baschong, C., Estrada, A.F., and Spang, A. (2014). The polysome-associated proteins Scp160 and Bfr1 prevent P body formation under normal growth conditions. J. Cell Sci. *127*, 1992–2004.

White, J.P., Cardenas, A.M., Marissen, W.E., and Lloyd, R.E. (2007). Inhibition of cytoplasmic mRNA stress granule formation by a viral proteinase. Cell Host Microbe *2*, 295–305.

Wilhelm, J.E., Buszczak, M., and Sayles, S. (2005). Efficient protein trafficking requires trailer hitch, a component of a ribonucleoprotein complex localized to the ER in Drosophila. Dev. Cell *9*, 675–685.

Wilhelmi, I., Kanski, R., Neumann, A., Herdt, O., Hoff, F., Jacob, R., Preußner, M., and Heyd, F. (2016). Sec16 alternative splicing dynamically controls COPII transport efficiency. Nat. Commun. *7*, 12347.

Yang, W.H., Yu, J.H., Gulick, T., Bloch, K.D., and Bloch, D.B. (2006). RNA-associated protein 55 (RAP55) localizes to mRNA processing bodies and stress granules. RNA *12*, 547–554.

Yonekawa, S., Furuno, A., Baba, T., Fujiki, Y., Ogasawara, Y., Yamamoto, A., Tagaya, M., and Tani, K. (2011). Sec16B is involved in the endoplasmic reticulum export of the peroxisomal membrane biogenesis factor peroxin 16 (Pex16) in mammalian cells. Proc. Natl. Acad. Sci. USA *108*, 12746–12751.

Zacharogianni, M., and Rabouille, C. (2013). Trafficking along the secretory pathway in Drosophila cell line and tissues: a light and electron microscopy approach. Methods Cell Biol. *118*, 35–49.

Zacharogianni, M., Kondylis, V., Tang, Y., Farhan, H., Xanthakis, D., Fuchs, F., Boutros, M., and Rabouille, C. (2011). ERK7 is a negative regulator of protein secretion in response to amino-acid starvation by modulating Sec16 membrane association. EMBO J. *30*, 3684–3700.

Zacharogianni, M., Aguilera-Gomez, A., Veenendaal, T., Smout, J., and Rabouille, C. (2014). A stress assembly that confers cell viability by preserving ERES components during amino-acid starvation. eLife *3*, e04132.

Cell Reports, Volume *20*

Supplemental Information

Phospho-Rasputin Stabilization by Sec16 Is Required for Stress Granule Formation upon Amino Acid Starvation

Angelica Aguilera-Gomez, Margarita Zacharogianni, Marinke M. van Oorschot, Heide Genau, Rianne Grond, Tineke Veenendaal, Kristina S. Sinsimer, Elizabeth R. Gavis, Christian Behrends, and Catherine Rabouille

Aguilera-Gomez et al, Cell Reports, 2017

Supplementary experimental procedures

Anti Rin antibody

The rabbit polyclonal anti-Rin was generated as follows: The *rin* coding region was PCR amplified from cDNA clone LD31994 (Berkeley *Drosophila* Genome Project) to add an NdeI site at the ATG and a BamHI site immediately following the stop codon. The PCR product was digested with NdeI and BamHI and inserted into the corresponding sites of pET15b. $(His)_6$-Rin was expressed in *E. coli* BL21 cells and then resolved by SDS-PAGE. The band corresponding to $(His)_6$-Rin was excised from the gel and used as the antigen to generate polyclonal rabbit anti-serum. The specificity of the antiserum was tested by immunoblotting of wild-type or rin^2/Df ovary extract and ECL detection. Anti-Rin was used at 1:500. The blot was re-probed with anti-Khc (1:20,000; Cytoskeleton) as a loading control (Suppl. Fig. S2D)

PMT-DNA constructs and dsRNAs

All the primers used for generating the DNA constructs and RNAi probes are listed in the Table below.

sfGFP-F	ggccgcggatggtgagcaagggcgagga
sfGFP-R	gggtttaaacttacttgtacagctcgtccatg
pMT- Rin -V5-F	cagtggtaccatggtcatggatgcgacccaatcg
pMT- Rin-V5-R	gtcaccgcgggcgacgtccgtagttgccaccac
pMT-Rin-S142A-V5-F	gaggacgagcaggatggcgaggcgcgatcggagaacgatgaggag
pMT-Rin-S142A-V5-R	ctcctcatcgttctccgatcgcgcctcgccatcctgctcgtcctc
pMT-Rin-S142E-V5-F	gaggacgagcaggatggcgaggagcgatcggagaacgatgaggag
pMT-Rin-S142E-V5-R	ctcctcatcgttctccgatcgctcctcgccatcctgctcgtcctc
pMT-Rin-d493-581-RRM-F	ttcggtgataat cgtgtccgcaacgacatggtgccgcgc
pMT-Rin-d493-581-RRM-R	gttgcggacacgattatcaccgaactgctgcgtgttgct
SEC16-SRD-F	cagtggtaccatgctgcagcaacagacgcgccc
SEC16-SRD-R	gtcaccgcggaatggggctgccatacgtttgcg
CAAX-RAS-F	cagtaccggttccggactcagatctcgagctc
CAAX-RAS-R	cagtgtttaaacttacataattacacactttgtctttgacttctttttc
CAAX-RAS-Sec16-F	cagtactagtatgttgcacaataatgcgccctggc
CAAX-RAS-Sec16-R	gtcaccgcggttgctggtgttgctgctgcagcg
SEC16>NC1-F	cagtactagtatgcattcaaccactcagcaggagaagaa
SEC16>NC1-R	ccaccggtaatggggctgccatacgtttgc
SEC16>CT-F	gtcaccgcggaaatgagacacgattaatgagaatgggatcatg
SEC16>CT-R	cagtggtaccatggcgagtcctccgaatgccactag
dsGFP-F	gggtttaaacttacttgtacagctcgtccatg
dsGFP-R	ggccgcggatggtgagcaagggcgagga
dsRin-F	taatacgactcactatagggccagacagattttcatagtgcg
dsRin-R	taatacgactcactatagggtggccatcattggatagctc
dsSec16-F	taataccgactcactatagggcgagatatggagcatttgacggagg
dsSec16-R	taatacgactcactatagggcgacttttctcgtgtggatgtgtgtg

To generate pMT-Rin-V5, Rin was amplified from S2 cells DNA and cloned into pMT-V5 using *SacII* and *KpnI*. To generate the mutant pMT-RinS142A, Rin cross-was amplified using primers harbouring a mutation at position S142A and cloned into pMT-V5 using *SacII* and *KpnI*. To generate the mutant PMT-Rin S142E Rin was cross-amplified using primers harbouring a mutation at position S142A and cloned into pMT-V5 using *SacII* and *KpnI*.

To generate the pMT-CAAX-sfGFP vector, the sequence corresponding to C-terminus CAAX motif of Ras (SGLRSRAQASNSRVKMSKDGKKKKKKSKTKCVIM) was

amplified and cloned into pMT-sfGFP using *AgeI* and *PmeI*. The Sec16 truncations: ΔNC1, ΔCter; Cter, SRD and Fl were cloned into pMT-CAAX-sfGFP using *EcoI* and *ApaI*.

To generate the pMT-sfGFP vector, super folder (sf) GFP was amplified and cloned into pMT-V5 using *SacII* and *PmeI* restriction sites replacing the V5 tag with sfGFP.

To generate the pMT Sec16 SRDC-sfGFP vector, SRDC was amplified from pMT Sec16fl GFP and cloned into pMT-sfGFP using *SacII* and *PmeI* restriction sites .

To generate the PMT-Rin-V5 ΔRRM, Ran was amplified using primers harbouring the RRM deletion (493-581aa) and cloned into pMT-V5 using KpnI and SacII.

The dsRNAs used for RNAi of Rin and Sec16 were amplified using primers harbouring T7 promoters in their sequence and used for *in vitro* transcription using the T7 Megascript Kit (AMBION) to generate the dsRNAs in the Table above.

Immuno-precipitation and mass spectrometry (MS/MS)

Sec16 immuno-precipitation: 200-300 million S2 cells were grown and starved in KRB for 4h. Cell lysate was prepared by incubating cells for 20 min on ice in lysis buffer (10% glycerol, 1% TritonX-100, 50mM TrisHCl pH 7.5, 150mM NaCl, 50mM NaF, 25mM Na_2-glycerophosphate, 1mM Na_2VO_4, 5mM EDTA, tablet protease inhibtors tablet (Roche). Protein A beads slurry was washed with lysis buffer and incubated for 1 hour at 4^0C with 20 ug of control IgG and anti Sec16 IgG. Subsequently, the beads where incubated for 2 hours at 4^0C with cell lysate. After washing with lysis buffer, beads where boiled for 10 min in sample buffer followed by SDS-PAGE and Western blot was performed.

Mass spectrometry: Endogenous Sec16 was immunoprecipitated from growing and starved S2 cells as described above and separated by SDS-PAGE. In-gel-trypsin digestion of the immunoprecipitates was performed as described previously (Shevchenko et al., 2006). Briefly, each lane was cut into five pieces and each piece was dehydrated with acetonitrile, reduced with DTT, alkylated with iodoacetamide and digested overnight with trypsin. Tryptic peptides were extracted with acetonitrile, desalted and analyzed by liquid chromatography tandem mass spectrometry (LC-MS/MS) using an Orbitrap Elite mass spectrometer coupled to a EasyLC nano-HPLC system (both Thermo Fisher Scientific, Dreieich, Germany). Peptide mixtures were loaded on a C18 reverse phase column in Solvent A (0.5% acetic acid) and eluted with a 5%-33% gradient solvent B (80% acetonitril in 0.5% acetic acid) running at a constant flow rate of 200 nl/min. Full-scan MS spectra were acquired in a mass range from m/z 300 to 2,000 with a resolution of 120.000 without lock mass. The 20 most intense precursor ions were sequentially CID fragmented in each scan cycle. In all measurements, up to 500 sequenced precursor masses were excluded from further analysis for 90 s. The target values of the mass analyzers were 1 million charges (MS) and 5,000 charges (MS/MS). The MS data was processed using default parameters of the MaxQuant software (1.5.3.8) (Cox and Mann, 2008). The peak lists were queried against the *Drosophila* UniProt database (2012_12). Full tryptic specificity was required, and up to two missed cleavages were allowed. Carbamidomethylation of cysteine was set as fixed modification. Protein N-terminal acetylation and oxidation of methionine were set as variable modifications. Initial precursor mass tolerance was set to 20 ppm and 0.5 Da at the fragment ion level. False discovery rates were set to 1% at peptide and protein group level.

To be scored as Sec16-interacting proteins, candidates were required to 1) be present in at least 2 experiments (out of 4 biological replicates) with at least 2 peptides per experiment and experimental conditions (growing and/or starvation) and 2) have an intensity of $\log_2$ (IgG:SEC16) ≥ 1 or in cases were proteins were not found in IgG control, have an intensity > 0. See Suppl Table 2 reporting the frequency of identification and the growth conditions. Both categories are color-coded and sortable.

Legends for Supplementary Figures and Tables

Suppl. Figure S1: Stress granules form upon amino-acid starvation and are distinct from autophagosomes (Related to Figure 1)
A-B: IF visualisation of FMR1 in cells incubated in culture medium (A), and KRB (A') supplemented or not with dialysed fetal bovine serum (FBS). Quantified in B.
Note that the absence of FBS does not lead to stress granule formation in cells incubated in culture medium. Conversely, note that the presence of FBS does not prevent stress granule formation in cells incubated in KRB (similar to **(Damgaard and Lykke-Andersen, 2011)** for HeLa cells). This demonstrates that the trigger of stress granule formation is amino-acid starvation.
C: Visualisation of the autophagosome marker Atg5-GFP and FMR1 in cells incubated in Schneider's and KRB for 3h. Note that stress granules and autophagosomes form upon starvation, but that they do not co-localise.

Suppl. Figure S2: Description of Rin, its domain and the anti-Rin rabbit polyclonal antibody (Related to Figure 2).
A: Comparison of the domain organisation in Rin and G3BP**.**
B: Ser142 in Rin is equivalent to Ser149 in G3BP. Drosophila Rin protein was used in a protein Blast against the NCBI NR database limited to eukaryotic sequences. The resulting 1704 protein sequences were used to generate a multiple sequence alignment. This analysis clearly showed that Ser149 from human G3BP directly aligns with the Drosophila Ser142 and that they are conserved.
C: Identification of the Rin RRM domain. Within the same alignment as described in B, 4 stretches of amino-acids in the region between Q493 and P581 (red boxes) were found highly conserved and correspond to RRM domains experimentally validated in G3BP.
D: The specificity of the Rin antiserum was tested by Western blotting of wild-type and rin^2/Df ovary extract and ECL detection. Anti-Rin was used at 1:500,000. The blot was re-probed with anti-Khc (1:20,000; Cytoskeleton) as a loading control. Note that the band at 75Kd disappears in the mutant extract.

Suppl. Figure S3: **Characterisation of Sec16 interaction with Rin (**Related to Figure 3).
A: WB visualisation of FRM1 and Caprin after Sec16 IP (after stripping of the blot shown in Figure 3D). FMR1 and Caprin do not appear to co-immunoprecipitate with Sec16.
B, B': Confocal section visualizating Rin-V5 (green) and Sec16 (red) after 0, 1, 2 h of amino-acid starvation. Sec16 and Rin increasingly appear to be in close proximity and overlapping. This interaction reaches its maximum at 2 h. Arrows point at Sec16 that is close to Rin. Quantified in C'.
C: Projection of 3 confocal sections co-visualising ΔNC1Sec16-GFP-CAAX and endogenous Rin (red) upon amino-acid starvation (KRB). Note that Rin is recruited to the plasma membrane
D: IF Visualisation of Rin ΔRRM-V5 (green) and FMR1 (red) in cells upon amino-acid starvation (KRB). Note that ΔRRM-V5 is not recruited to stress granules and also largely prevents their formation (arrowhead), whereas stress granules form normally in non-transfected cells.

Suppl. Figure S4: stress granule formation in DTT and heat shock (Related to Figure 4)

A: IF visualization of endogenous FMR1 in mock- and Sec16 depleted cells upon heat shock (3h) and DTT (3h). Note that stress granules form as efficiently in mock and Sec16 depleted cells.
B: IF visualization of FMR1 in mock- and Sar1 depleted cells incubated in KRB for 4h. Note that stress granule formation is as efficient in both depletions. Note that the Sar1 depletion was evidenced by the typical enlargement of the ERES **(Ivan et al., 2008).**
C: IF visualization of FMR1 in cells treated or not with BFA. Note that stress granule formation is as efficient in treated and non-treated cells.
Scale bars: 10 µm

Suppl. Figure S5: Stress granules formation in Sec16 depleted cells (Related to Figure 5)
A: Rin PCR product in mock and Sec16 depleted cells in growing conditions (Sch) and upon amino-acid starvation (KRB). Note that the level is similar. H2A acts as the control mRNA.
B: IF visualisation of Rin-V5 (green) and FMR1 (red) in mock- and Sec16 depleted transfected cells incubated in KRB supplemented or not with MG132. Note that MG132 incubation rescues Rin-V5 level in Sec16 depleted cells as well as the formation of stress granule formation in transfected cells (Rin-V5 and FMR1 positive, arrow).

However, whereas stress granules form in non-transfected mock-depleted cells upon KRB (double arrows, as shown in Figure 5D), stress granules do not form in non-transfected Sec16 depleted cells, even in the presence of MG132 (arrowhead). This clearly shows that Sec16 is needed for stress granule formation, not only for Rin recruitment.

Cox, J., and Mann, M. (2008). MaxQuant enables high peptide identification rates, individualized p.p.b.-range mass accuracies and proteome-wide protein quantification. Nature biotechnology *26*, 1367-1372.
Damgaard, C.K., and Lykke-Andersen, J. (2011). Translational coregulation of 5'TOP mRNAs by TIA-1 and TIAR. Genes & development *25*, 2057-2068.
Ivan, V., de Voer, G., Xanthakis, D., Spoorendonk, K.M., Kondylis, V., and Rabouille, C. (2008). Drosophila Sec16 mediates the biogenesis of tER sites upstream of Sar1 through an arginine-rich motif. Molecular biology of the cell *19*, 4352-4365.
Shevchenko, A., Tomas, H., Havlis, J., Olsen, J.V., and Mann, M. (2006). In-gel digestion for mass spectrometric characterization of proteins and proteomes. Nature protocols *1*, 2856-2860.

Supplementary Figure S1: Aguilera-Gomez et al, 2017

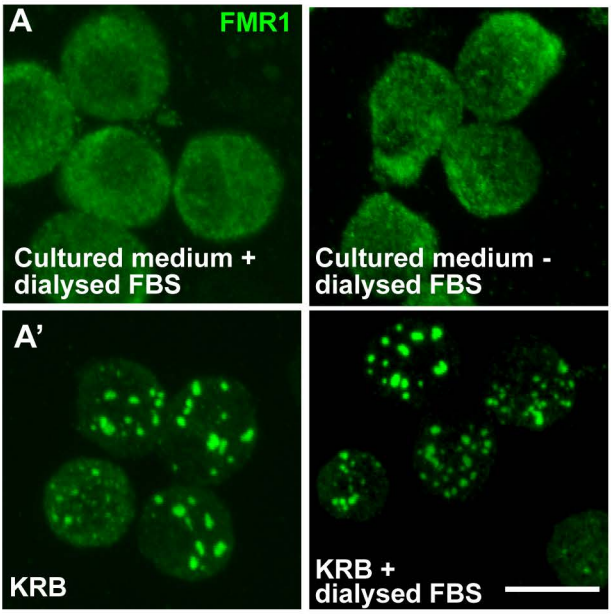

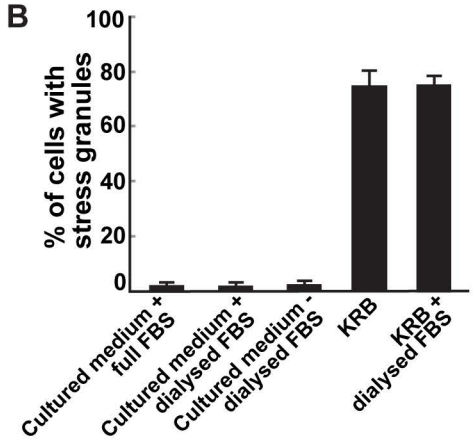

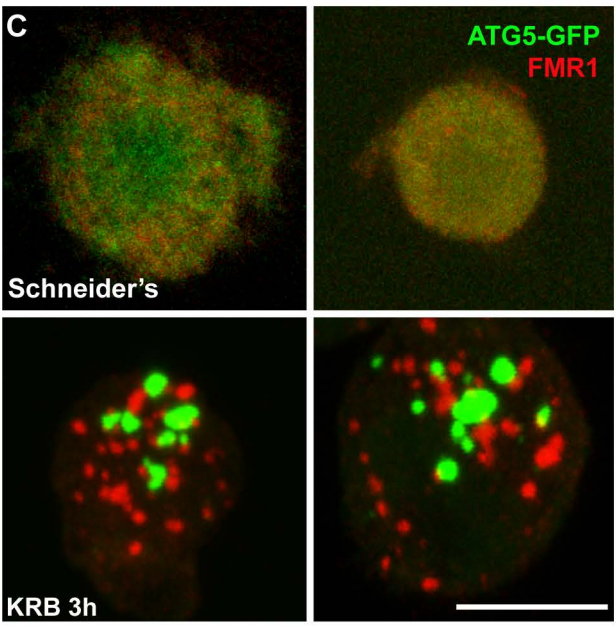

Supplementary Figure S2: Aguilera-Gomez et al, 2017

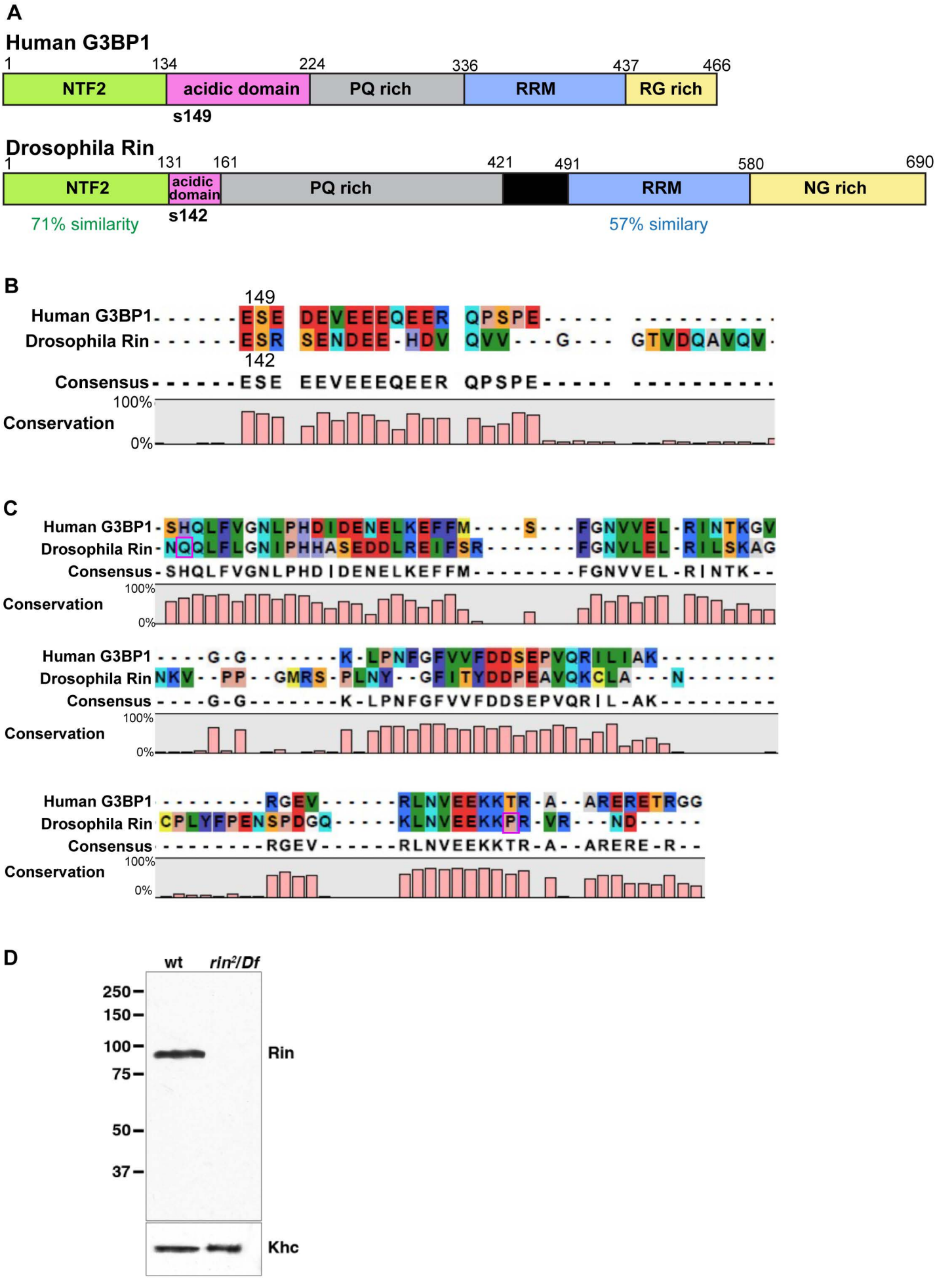

Supplementary Figure S3: Aguilera-Gomez et al, 2017

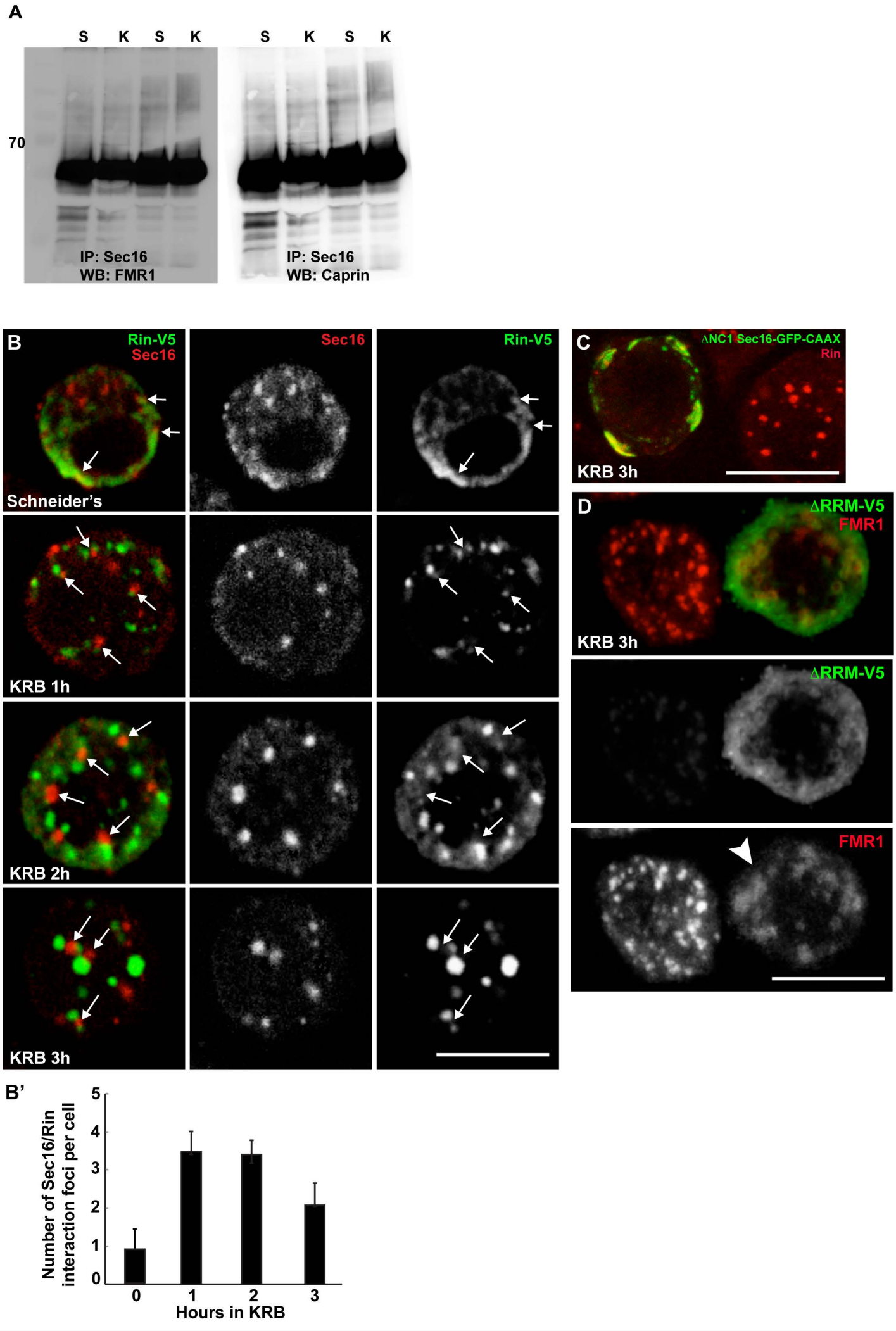

Supplementary Figure S4: Aguilera-Gomez et al, 2017

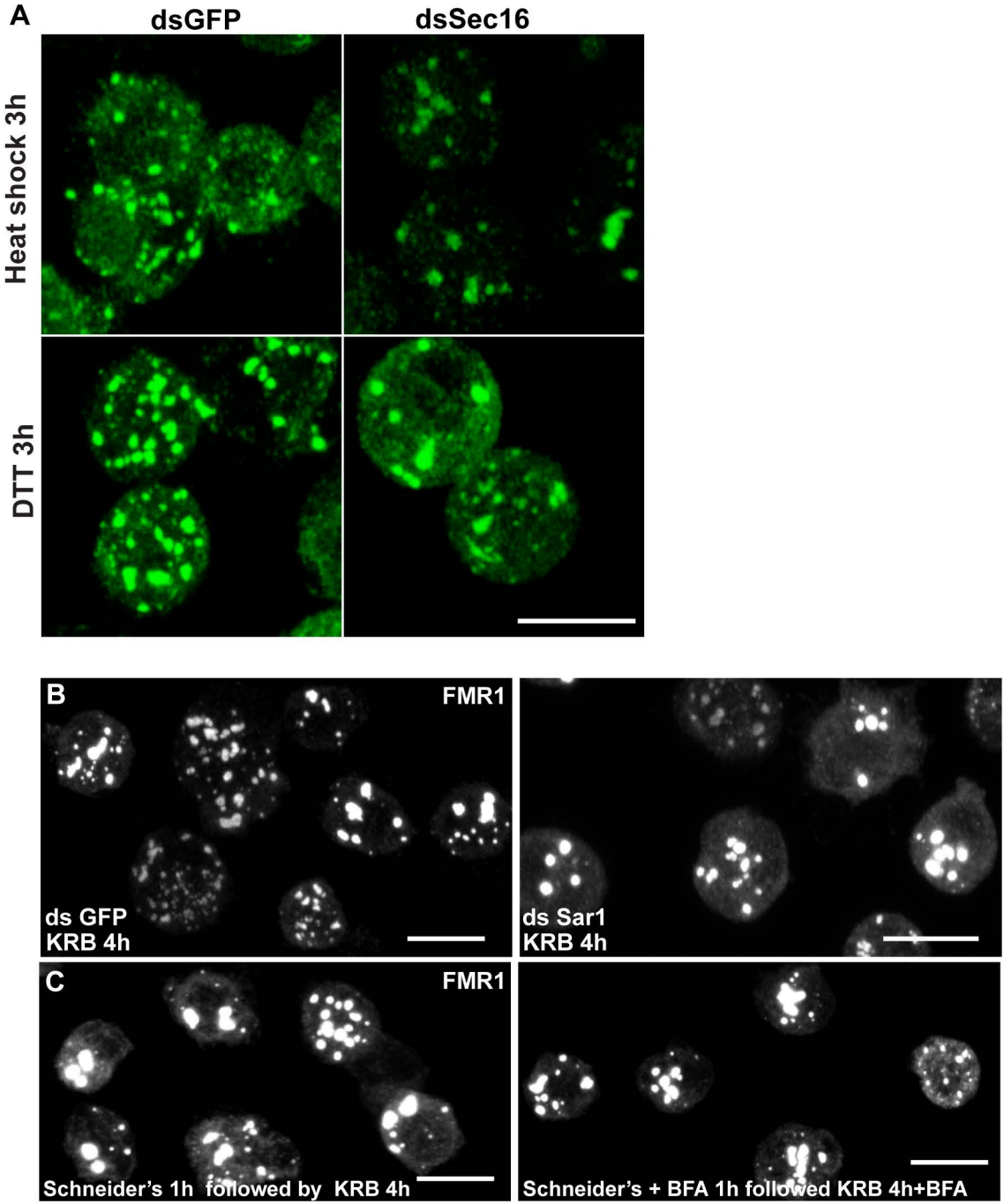

Supplementary Figure S5: Aguilera-Gomez et al, 2017

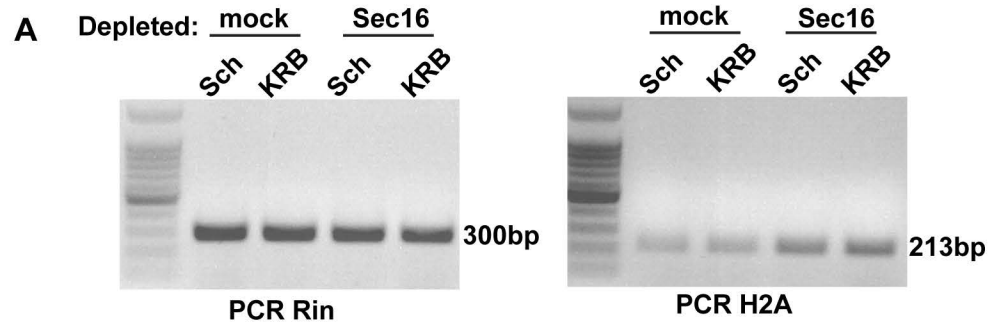

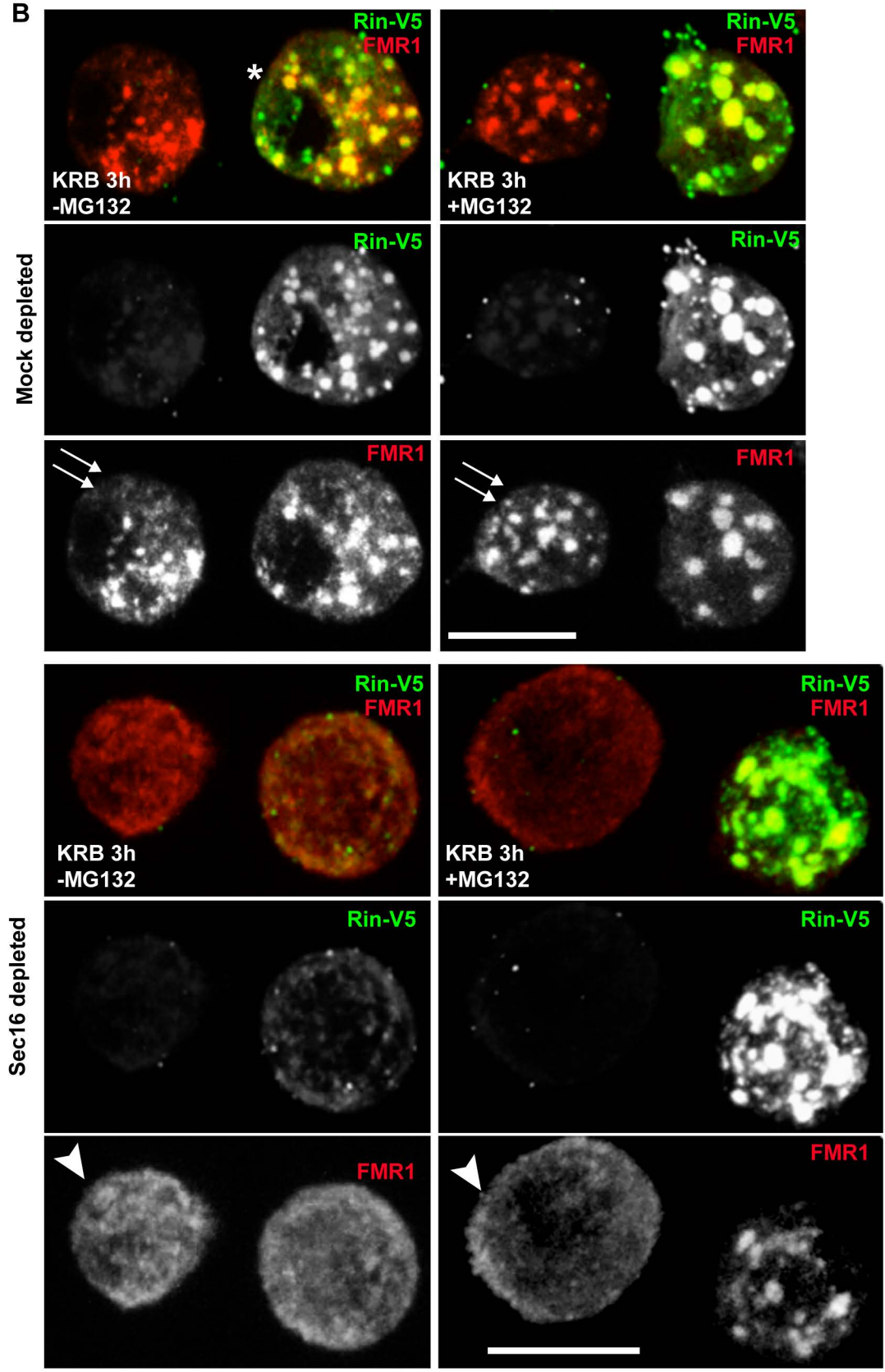

Supplementary Table S1

	Stress granules upon amino-acid starvation	Size	Number per cell
1	Endogenous	650±350 nm	11±6
2	Endogenous in S142A-V5 transfected cells	662 nm±100	29±5
3	Rin-V5 positive upon expression in wild type cells	751±120 nm	26±7
4	S142E-V5 positive upon expression in wild type cells	1000±60 nm	15±5
5	Rin-V5 positive upon expression in Rin depleted cells	630 nm	34±8
6	Reversion in full medium 3h	0	0
7	S142E-V5 positive upon expression in Rin depleted cells	1100±100 nm	17±4
8	Reversion in full medium 3h	640±90	33±6